Fakultät für Medizin

Abteilung für diagnostische und interventionelle Neuroradiologie

Using magnetic resonance spectroscopy to study neural activity: The role of inhibitory and excitatory neurotransmitters for systems-level brain dynamics

Katarzyna Kurcyus

Vollständiger Abdruck der von der Fakultät für Medizin der Technischen Universität München zur Erlangung des akademischen Grades eines

Doctor of Philosophy (Ph.D.)

genehmigten Dissertation.

Vorsitzender: Prof. Dr. Arthur Konnerth

Betreuer: Priv.-Doz. Dr. Valentin Riedl

Prüfer der Dissertation:

1. apl. Prof. Dr. Helmut Adelsberger

2. Prof. Dr. Markus Ploner

Die Dissertation wurde am 30.06.2017 bei der Fakultät für Medizin der Technischen Universität München eingereicht und durch die Fakultät für Medizin am 14.07.2017 angenommen.

Summary

Magnetic resonance spectroscopy (MRS) is an emerging technique to study metabolites in the human brain. A novel, edited MRS method allows to quantify the concentration of most abundant inhibitory and excitatory neurotransmitters: γ-aminobutyric acid (GABA) and glutamate (Glu). This approach revealed altered levels of neurotransmitters in pathological brain states (such as depression and schizophrenia) but the relationship of neurotransmitter levels to neuronal activity and behaviour is still unclear.

Crucially, studies have focused so far on the influence of baseline neurotransmitter levels on fMRI (functional magnetic resonance imaging) activity or behavioural performance, but did not investigate these relationships during identical conditions. Moreover, studies have never analysed both neurotransmitters, GABA and Glu, during identical states.

In this thesis, I focus on the visual system in the healthy brain and study the relationship of both GABA and Glu with fMRI activity and visual performance during different behavioural states. I also investigate whether non-invasive brain stimulation allows to intentionally modulate neurotransmitter levels and might therefore be tested as a therapeutic tool.

I started by establishing an acquisition and analysis pipeline for edited MRS on two MR scanners in order to separately quantify GABA and Glu neurotransmitters in the human brain. This procedure included the evaluation of scanning parameters, the assessment of regions of interest, and the optimization of signal-to-noise ratio of separate acquisitions. This unique and technically demanding method implemented in our research laboratory is now ready for use in further studies.

The goal of Experiment 1 was to systematically investigate GABA and Glu neurotransmitter concentrations in the visual cortex in different brain states, and to

relate them to the most typical measures in cognitive neuroscience, fMRI activity and visual performance. Three brain states were studied with increasing visual input: eyes closed state (CLOSED) with no input, eyes open state (OPEN) during darkness with weak input, and the visual stimulation state (VIS STIM) with strong flickering chequerboard presentation. I found opposite changes of neurotransmitters along brain states with GABA decreasing from CLOSED to OPEN and Glu increasing from CLOSED to VIS STIM. Furthermore, GABA correlated inversely with the visual performance. This is the first report of systematic changes of excitatory and inhibitory neurotransmitters across healthy brain states. Moreover, these results might explain the inconsistent findings in previous studies as both neurotransmitters change differently along brain states.

The goal of Experiment 2 was to systematically investigate the effects of non-invasive brain stimulation on the neurotransmitter concentrations in the occipital cortex. Stimulation to a distant yet connected brain region modified GABA but not Glx concentration in the occipital cortex and affected the fMRI measures within and outside of the visual system.

In summary, this thesis addresses two questions:

- Do neurotransmitter concentrations reflect behavioural states and visual performance?
- Can we modulate neurotransmitters in the visual system with non-invasive brain stimulation?

Zussamennfassung

Diese Dissertation untersucht die Rolle der wichtigsten inhibitorischen und exzitatorischen Neurotransmitter - GABA und Glutamat - im visuellen System. Die Kombination zweier Methoden: Magnetresonanzspektroskopie (MRS) und funktionell Magnetresonanztomographie (fMRT), erlaubte es, die Neurotransmitterlevel mit der neuronalen Aktivität zu verknüpfen. Darüber hinaus untersuchten wir die Auswirkungen der transkraniellen Magnetstimulation auf die Neurotransmission, sowie auf das fMRT.

Legal information

The results of Experiment 1 of this dissertation have been partially published under following reference:

Katarzyna Kurcyus, Efsun Annac, Nina M. Hanning, Ashley D. Harris, Georg Oeltzschner, Richard Edden, Valentin Riedl. Opposite dynamics of GABA and glutamate levels in the occipital cortex during visual processing. *J Neurosci*, 2018, Oct 3, pii: 1214-18. doi: 10.1523/JNEUROSCI.1214-18.2018

The results of Experiment 2 of this dissertation are in the preparation for publication at the submission date of this thesis.

Contents

I Introduction **14**

1 Magnetic resonance spectroscopy **15**

2 MEGA-PRESS spectroscopy **17**

3 GABA and GABAergic neurotransmission **19**

4 Glutamate and glutamatergic neurotransmission **21**

5 Blood-oxygen-level dependent signal **21**

6 Transcranial magnetic stimulation **26**

II Aims and hypotheses **27**

III Materials and methods **28**

1 Participants and study design **28**

1.1 Experiment 1 28

1.2 Experiment 2 29

2 Data acquisition **31**

2.1 Magnetic resonance spectroscopy 31

2.1.1 Siemens 31

2.1.2 Philips 32

2.2 Other magnetic resonance methods 33

2.2.1 Siemens . . . 33
2.2.2 Philips . . . 34
2.3 Transcranial magnetic stimulation . . . 34
2.4 Behavioural experiments . . . 35
2.4.1 Orientation discrimination experiment . . . 36
2.4.2 Attentional capture experiment . . . 37

3 Data analysis 40
3.1 Magnetic resonance spectroscopy . . . 40
3.1.1 Siemens . . . 41
3.1.2 Philips . . . 43
3.2 fMRI . . . 43
3.3 Behavioural experiments . . . 47
3.3.1 Orientation discrimination . . . 47
3.3.2 Attentional capture . . . 47
3.4 Statistical analysis . . . 48

IV Results 49

1 The role of GABA and Glx in the visual system. 49
1.1 GABA and Glx concentration in different brain states . . . 49
1.2 Concentration of other metabolites in different brain states . . . 56
1.3 fMRI measures in different brain states . . . 57
1.4 Relationship between local and distal neuronal activity, and neurotransmitters concentration . . . 60
1.5 Results of behavioural experiments . . . 64

1.6 Relationship between behaviour and neurotransmitters concentration . . . 65

1.7 Relationship between behaviour and fMRI measures 66

2 Modulation of neurotransmitters by TMS 68

2.1 Modulation of GABA and Glx by the TMS intervention 68

2.2 Modulation of other metabolites by the TMS intervention 74

2.3 fMRI measures before and after the rTMS 75

V Discussion 78

1 The role of GABA and Glu in the visual system. 78

1.1 Changes in GABA and Glx across brain states 78

1.1.1 GABA decreases from CLOSED to OPEN states with no further change during VIS STIM 78

1.1.2 Glx increases from CLOSED to VIS STIM states 81

1.1.3 Control analyses 82

1.2 Relationship between neuronal activity and neurotransmitter concentrations 83

1.2.1 Baseline GABA concentrations and ongoing neuronal activity . . . 83

1.2.2 Task related increase of Glx concentrations and local neuronal activity 84

1.3 Relationship between behaviour and neurotransmitters concentrations . . . 85

1.4 Study limitations 86

2 Experiment 2. Modulation of neurotransmitters by TMS 87

2.1 TMS intervention modulates GABA concentration 88

2.2 Modulation of local and distal neural activity by TMS 90

2.3 Study limitations 91

VI Conclusions and Outlook 92

VII Publications 109

1 Publications derived from this thesis 109

2 Publications, which are not part of this thesis 109

3 Oral presentations derived from this thesis 110

4 Poster presentations derived from this thesis 110

VIII Acknowledgements 112

List of Tables

1 Individual resting state motor threshold (rMT) 35

2 Group averaged GABA+/Cr and Glx/Cr concentrations in Experiment 1. 50

3 Group averaged FWHM scores of GABA and Glx peaks in Experiment 1. . 54

4 Shapiro test results in Experiment 1 55

5 Correlation coefficients between GABA+/Cr and Glx/Cr in Experiment 1 55

6 Group averaged metabolites concentrations in the "edit-off" spectrum in Experiment 1 56

7 fMRI group results in Experiment 1 58

8 Individual fMRI results in Experiment 1 59

9 Group averaged spectroscopy results in Experiment 2. 69

10 Group averaged metabolite concentrations in the "edit-off" spectrum in Experiment 2 75

List of Figures

1 Metabolites quantified with the PRESS MRS signal 16

2 The foundation of MEGA-PRESS method. 18

3 Schematic depiction of the GABA cycle. 20

4 Schematic depiction of the glutamate cycle. 22

5 The haemodynamic response and fMRI BOLD signals. 23

6 A 7-network parcellation of the human cerebral cortex. 25

7 Scheme of MRS and fMRI experimental sessions in the Experiment 1. . . . 29

8 Sequence of events in the Experiment 2 and the depiction of areas stimulated with the rTMS 30

9 MRS voxel placement in the occipital cortex in the saggital and axial plane. 32

10 Orientation discrimination task scheme. 37

11 Attentional capture task scheme 39

12 Sample fits of the edited and "edit-off" spectra. 41

13 Assessment of the spectroscopy data quality in Experiment 1 42

14 Assessment of the spectroscopy data quality in Experiment 2 44

15 Concentrations of metabolites in the visual cortex in CLOSED and OPEN conditions: data concatenated from both cohorts. 51

16 Concentrations of metabolites in the visual cortex in CLOSED, OPEN, and VIS STIM conditions. 52

17 Results of group BOLD signal changes 60

18 Local neuronal activity and concentrations of neurotransmitters in Experiment 1 62

19 Functional connectivity and concentrations of neurotransmitters in Experiment 1 63

20 Relationship between the BOLD signal change and neurotransmitters concentration in Experiment 1 64

21 Relationship between visual sensitivity and neurotransmitters concentration 66

22 GABA/H_2O concentration distribution before and after TMS intervention 70

23 GABA/Cr concentration distribution before and after TMS intervention . 71

24 Glx/Cr concentration distributions before and after the TMS intervention . 72

25 Relationship between GABA/Cr and Glx/Cr concentration after the TMS intervention in the angular gyrus. 74

26 Modulation of network connectivity after the TMS intervention 77

27 Depiction of GABA/glutamate and glutamine circle 80

List of abbreviations

3T	3-Tesla magnetic resonance scanner/system
7T	7-Tesla magnetic resonance scanner/system
AG	angular gyrus
AP	action potential
Asp	aspartate
ATP	Adenosine triphosphate nucleoside
BOLD	blood-oxygen-level dependent signal
CLOSED	session performed with eyes closed
CSF	cerebrospinal fluid
DAN	dorsal attention network
deg	degrees
DMN	default mode resting state network
EEG	electroencephalography
EPI	echo-planar imaging
fMRI	functional magnetic resonance imaging
FOV	field of view
FWHM	full width at half maximum
GABA	gamma-aminobutyric acid
$GABA_A$	A-type GABA receptor
$GABA_B$	B-type GABA receptor
GAD	glutamate decarboxylase
GAT	GABA transporter proteins
Gln	glutamine

Glu	glutamate
GABA+	GABA signal with a contribution from macromolecules
Glx	combined glutamate and glutamine signals mainly derived from glutamate
PCh	phosphocholine
GSH	glutathione
ICA	independent component analysis
iFC	intrinsic functional connectivity
Ins	myo-inositol
IPL	ipsolateral inferior parietal lobus
iTBS	inhibitory theta-burst transcranial stimulation
lAG	left angular gyrus
MEGA-PRESS	Mescher-Garwood point-resolved spectroscopy
MPRAGE	magnetization prepared rapid acquisition gradient echo
MRI	magnetic resonance imaging
MRS	magnetic resonance spectroscopy
NAA	N-Acetylaspartate
OPEN	session performed with eyes open
PAG	phosphate-activated glutaminase
PET	positron emission tomography
PFC	prefrontal cortex
post-TMS	session performed after TMS intervention
ppm	particles per million
pre-TMS	session performed before TMS intervention
RF pulse	radiofrequency pulse

rMT	resting motor threshold
rs-fMRI	resting-state functional magnetic resonance imaging
RSN	resting-state network
RT	reaction time
rTMS	repeated TMS
SNR	signal-to-noise ratio
SVS	single voxel spectroscopy
TCA cycle	tricarboxylic acid cycle
TE	echo time
TMS	transcranial magnetic stimulation
TR	repetition time
VIS STIM	session performed during visual stimulation is applied

Part I

Introduction

The balance of excitation and inhibition is a key feature of normal brain function. γ-aminobutyric acid (GABA) and glutamate (Glu) are two most important neurotransmitters involved in this process. Magnetic resonance spectroscopy (MRS) is a promising method to study these molecules *in vivo*. Yet, it is not completely clear which levels of neural activity the MRS captures.

In the first experiment of this thesis, I studied the dynamics of GABA and Glu concentrations in the visual system across different brain states. I also established a relationship between neurotransmitter concentrations and neuronal activity as measured with functional magnetic resonance imaging (fMRI) during the same brain states. Finally, I addressed the question whether neurotransmitter levels in the visual system predict visual performance.

In a second set of experiments, I studied whether neurotransmitter concentrations in the visual system can be modulated by non-invasive brain stimulation. Several studies showed altered levels of GABA and Glu in neuropsychiatric disorders. In the second part of the thesis, I therefore explore the feasibility of brain stimulation as a therapeutic tool to modulate the balance of excitatory and inhibitory neurotransmitters in the human brain.

1 Magnetic resonance spectroscopy

MRS is a non-invasive technique to measure metabolite concentrations in a tissue *in vivo* using an MR scanner. Its clinical use in the field of neuroradiology includes examination of metabolic changes in tumours, regions affected by stroke, neurodegenerative and psychiatric diseases. Outside of the central nervous system, MRS is an important tool to diagnose muscle disorders and to monitor their development [110].

MRS spectra can be acquired from diverse atoms, including phosphorus (31P), carbon (13C) and hydrogen (1H). While phosphorus and carbon spectroscopy study cells' respiratory and energetic processes, proton spectroscopy investigates myelin, markers of neural functioning (among them neurotransmitters), metabolically active components and cell membranes [110].

The MRS signal can be acquired from a single voxel (SVS – single voxel spectroscopy) or a multi-voxel region (CSI or MRSI – chemical shift imaging or multivoxel spectroscopy). In the SVS method, typical sequences include PRESS and STEAM, both employing short-TE (short echo-time). The PRESS pulse sequence detects metabolites including the neuron marker N-acetyl-aspartate (NAA), structural compounds like choline (Cho), creatine (Cr) and phosphocreatine (PCr), the neural activity marker aspartate (Asp), the oxidative stress marker glutathione (GSH) and the astrocyte marker myo-inositol (Ins) [95], see Figure 1.

In this thesis, a modified version of SVS 1H-PRESS pulse sequence was employed to study neurotransmitter concentrations. Details of this method are described in the next section.

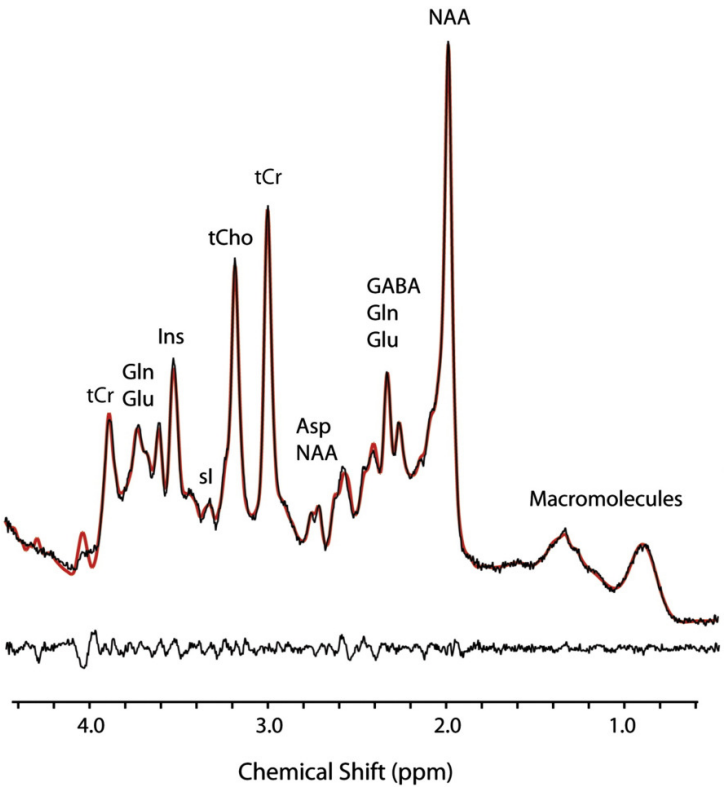

Figure 1: Metabolites measured with the PRESS MRS signal: N-acetyl-aspartate (NAA) at 2.0 ppm or 2.0.3 ppm; choline (Cho) at 3.2 ppm; creatine (Cr) and phosphocreatine (PCr) at 3.0 ppm; lactate (Lac) at 1.3 ppm; lipid signals at 0.9-1.3 ppm; glutamate (Glu) and glutamine (Gln), usually found as a duplex (Glx) at 2.2-2.4 ppm and 3.5-4 ppm; myoinositol (Ins) at 3.6 ppm; ppm – particles per million. Adapted from [95]

2 MEGA-PRESS spectroscopy

A recently developed extension of the 1H-PRESS sequence allows to differentiate neurotransmitters from the MRS-spectrum, which has not been possible with standard MRS sequences so far. This MEGA-PRESS (MEscher–GArwood-Point RESolved Spectroscopy) method uses J-difference editing to resolve GABA and Glu peaks from the spectrum [81].

The GABA and Glu peaks, covered in the PRESS spectrum by creatine and choline, are separated in the MEGA-PRESS sequence by the scalar coupling process, which is defined as the interaction between hydrogen nuclei within a molecule. During measurements, a radiofrequency pulse (RF pulse) is applied to one of the coupled hydrogens, causing an alteration in the spin of its partner (hydrogen) and thereby uncovering the peak of interest [29]. In this technique, two interleaved datasets are acquired. The first dataset is edited with the pulse at 1.9 ppm with the aim to refocusing the J-coupling spins at 3 ppm (the "ON" spectrum). In the other dataset, a regular RF pulse is applied (the "OFF" spectrum). The subtraction of "ON" from "OFF" spectra removes all the peaks that were not affected by the editing procedure and allows the quantification of GABA and Glx (combined glutamate and glutamine signals mainly derived from the glutamate molecule), see Figure 2. Since the two types of spectra are acquired in an interleaved fashion, the subtraction is done as a post-processing step of the data analysis. In order to increase the acquired data quality, the movement and scanner drift corrections are incorporated in the MEGA-PRESS pulse sequence.

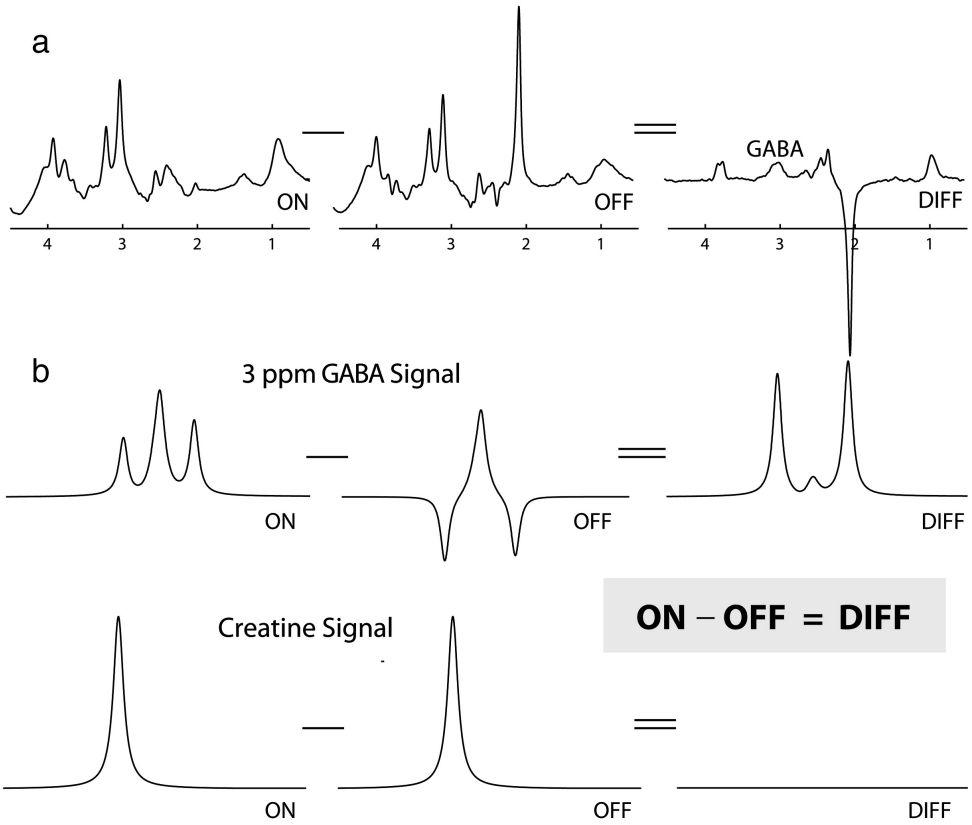

Figure 2: The foundation of MEGA-PRESS method. (a) Editing pulses are applied at 1.9 ppm to uncover the GABA peak at 3 ppm (b). Non-edited scans (OFF) are subtracted from edited ones (ON) and the difference spectrum (DIFF) is computed. The edited spectrum contains signals close to 1.9 ppm (directly affected by the pulses), the GABA signal at 3 ppm, the combined glutamate+glutamine (Glx) peak at 3.75 ppm, and J-coupled macromolecular (MM) peaks. Adapted from [84]

3 GABA and GABAergic neurotransmission

GABA is the major inhibitory neurotransmitter in the human brain involved in both local and long-axoned brain projections [31]. GABA plays an important role in such physiological processes as sleep, motor control and pain. Defects in GABAergic transmission relate to epilepsy, anxiety and psychiatric and neurodegenerative disorders [98].

GABA is produced from glucose via the α-ketoglutarate molecule derived in the tricarboxylic acid cycle (TCA) by the enzyme glutamic acid decarboxylase (GAD). GAD is exclusively localized in the neurons that use GABA as a neurotransmitter [31]. A major source of neurotransmitter synthesis is astrocytic glutamine (Gln), as transport blockage of this compound reduces GABA concentration [90, 91, 97]. A depiction of the GABA cycle can be found in Figure 3.

$GABA_A$ and $GABA_B$ are two main receptors that respond to the neurotransmitter. Both are found pre- and post-synaptically throughout the brain [98]. Modulation of GABA receptors causes either an increase or a decrease in GABA transmission because it depends on the amount of the generated inhibitory activity [86, 87]. Once released into the synaptic cleft, GABA is taken up by the neurons and glial cells with one of four types of GABA transporter proteins (GAT) that inactivate and regulate GABAergic neurotransmission [31].

GABA is more abundant in gray matter than in white matter [22] and is found in three main pools: in the cellular cytoplasm, inside cellular vesicles, and in the synaptic cleft. Current research suggests that GABA MRS captures the signal from the synaptic cleft pool [112].

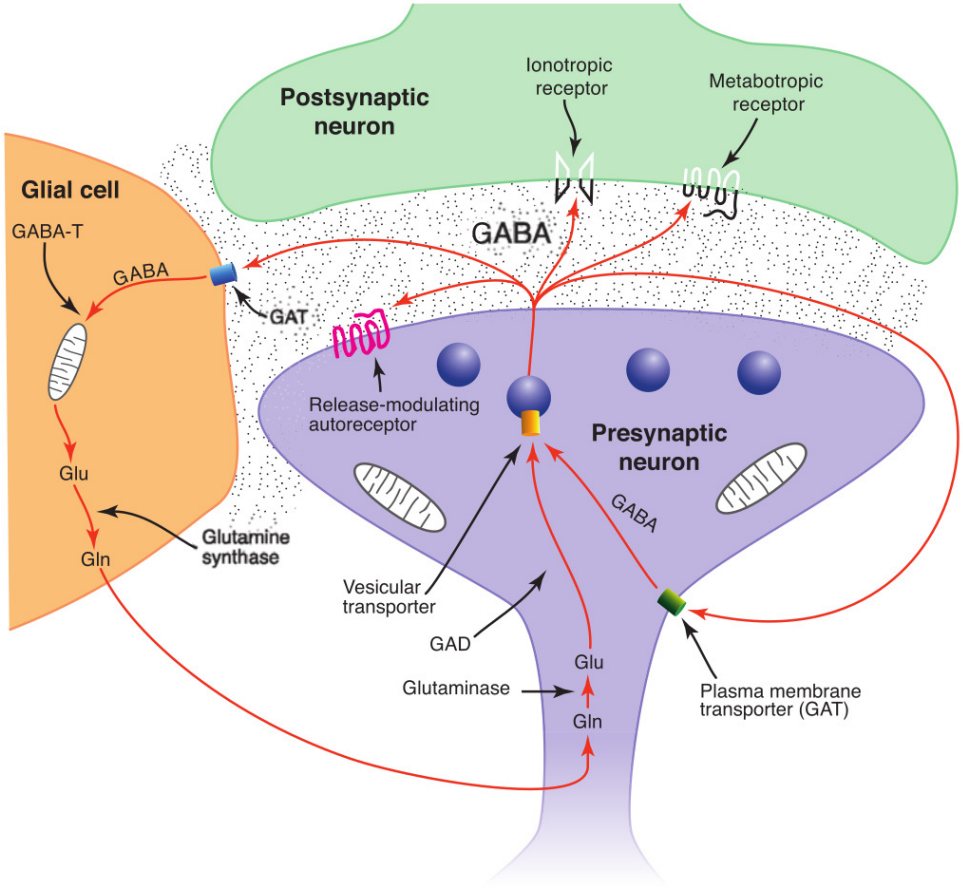

Figure 3: Schematic depiction of the GABA cycle. α-ketoglutarate formed in the Krebs cycle is transaminated to Glu by GABA transaminase (GABA-T). The transmitter GABA is formed from the Glu by glutamic acid decarboxylase (GAD). GABA released into the extracellular space of the synapse is taken up by high-affinity GABA transporters (GAT) found on neurons and glia. Adapted from[31]

4 Glutamate and glutamatergic neurotransmission

Excitatory amino acid transmitters are responsible for most of the fast synaptic transmission in the central nervous system. Glu, a major excitatory brain neurotransmitter [39], is synthesized locally in nerve terminals (from glucose in the TCA cycle via α-ketoglutarate) or from Gln in glial cells. In the indirect Glu synthesis, Gln is transported from astrocyte to neuron, and transformed to Glu by glutaminase (PAG) [31]. A depiction of the glutamate cycle can be found in Figure 4.

A depolarisation of the nerve terminal releases Glu in a calcium-dependent manner. Once released to the synaptic cleft, the neurotransmitter is being reuptaken to neurons and glial cells by its ionotropic (NMDA, AMPA and Kainate) or metabotropic (MGluR) receptors [27, 63]. There are at least eight types of metabotropic receptors identified suggesting that the glutamatergic neurotransmission must display many critical functions [31].

Since glutamate molecule may participate in both cellular communication and metabolic processes, it is difficult to clearly explain fluctuations in its concentration [31]. However, in most brain cells the Glu pool is mainly related to the neurotransmission [65]. In particular, the MRS-derived Glu signalling in the visual cortex strongly correlated with the visual stimulation [74, 103].

5 Blood-oxygen-level dependent signal

Glucose and oxygen are the key substrates of energy supply for the brain. fMRI indirectly identifies areas of neuronal activity via changes in oxygen supply. Neuronal activity leads to vasodilatation of surrounding capillaries and to an increased oxygen supply via

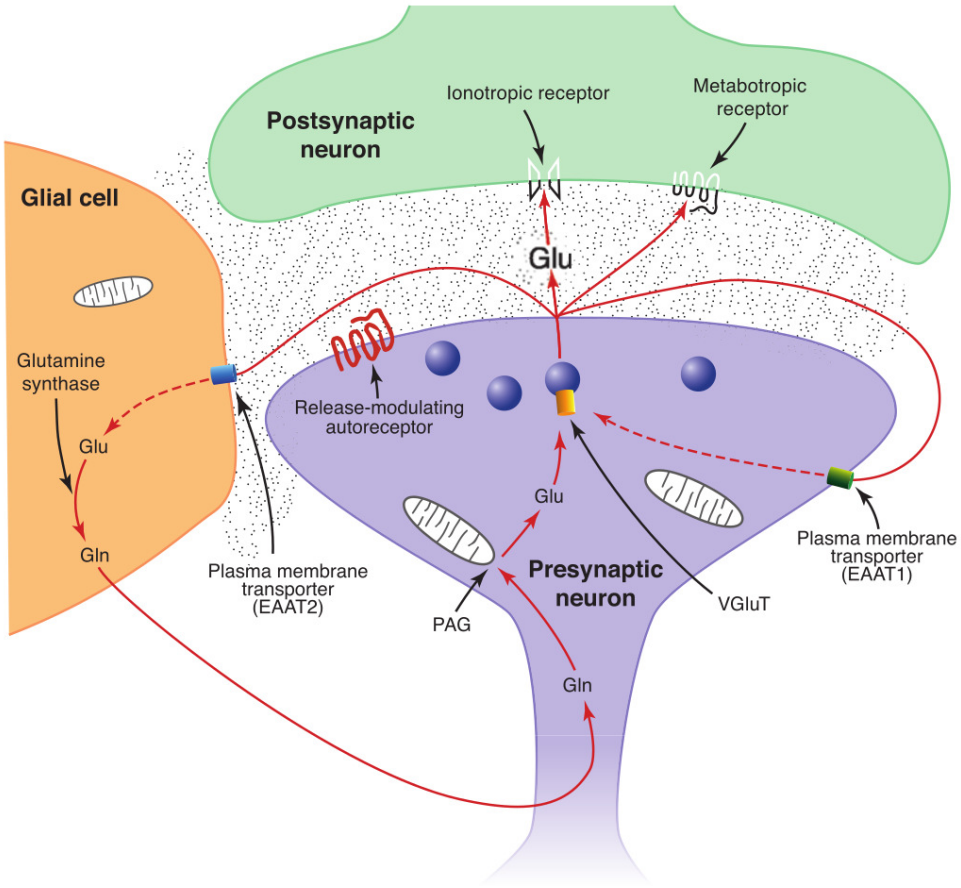

Figure 4: Schematic depiction of the glutamate cycle. Glu is packed by a vesicular transporter into vesicles. After release from the presynaptic terminal, Glu can interact with postsynaptic and/or release-modulating receptors. Glutamate is then taken up from the synaptic region by the high-affinity plasma membrane transporters or by recycling through adjacent glia. Adapted from [31]

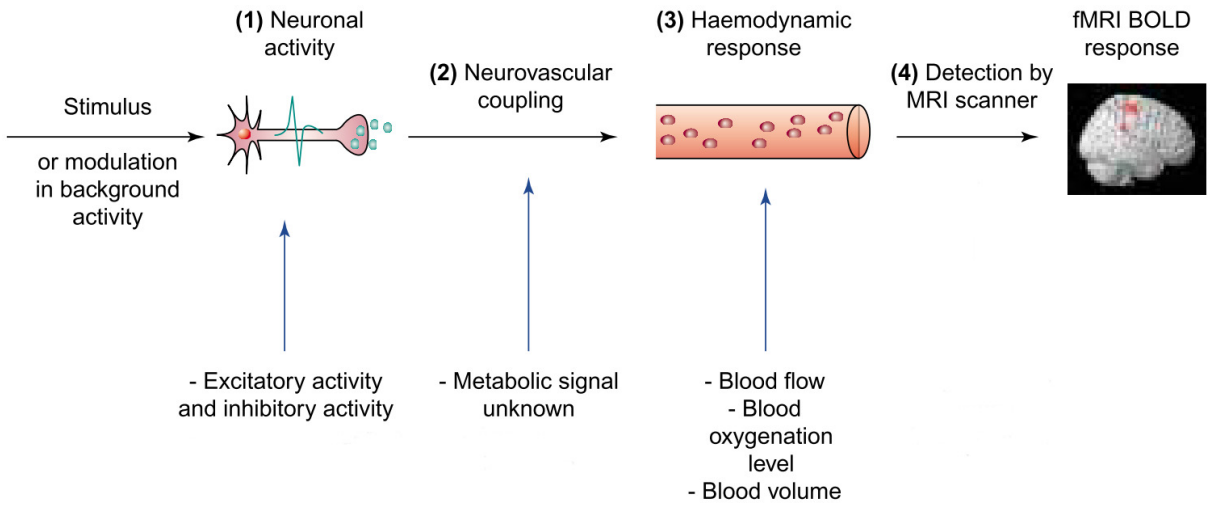

Figure 5: The haemodynamic response and fMRI BOLD signals. The BOLD signal has several components: (1) the neuronal response to a stimulus or background modulation; (2) the process of coupling neuronal excitatory and inhibitory activity with a haemodynamic response (neurovascular coupling); (3) the haemodynamic response; and (4) the method of detecting this response by an MRI scanner. Adapted from [2]

haemoglobin. fMRI is sensitive to changes in haemoglobin concentrations. An increase in the fMRI signal, the so-called blood-oxygen-level dependent (BOLD) signal, thereby indirectly identifies brain regions of increased neuronal activity [7, 13, 28, 79, 93], see Figure 5.

Changes in BOLD signal can be investigated during a task (task-fMRI) or at rest (resting-state fMRI; rs-fMRI). Task-fMRI studies identify brain regions of increased BOLD-signal while subjects perform a cognitive task in the scanner [71]. Rs-fMRI identifies signal fluctuations related to ongoing brain activity in the resting state.

Amplitude of low-frequency fluctuations. ALFF is a measure of spontaneous low-frequency fluctuations in the BOLD signal; its role as a biomarker was extensively investigated in the last decade. Changes in the ALFF at rest were reported in ageing processes

[125], as well as in the course of such diseases as schizophrenia [51, 53], ADHD [129] and Parkinsonism [126]. Alterations in the ALFF were associated with pathologies distributed across the brain [30]; sleep deprivation was found to temporally impair ALFF scores [41].

Seed-based functional connectivity (seed-based FC). FC is a measure of synchronized fMRI signal fluctuations in distinct brain regions. If the signal from a seed area is correlated in time with a distant brain regions, these regions are likely to communicate and share information [106]. With the seed-based FC, cognitive skills may be assessed, i.e. Broca's area and Brodmann's area 39 were found to correlate with reading abilities [46]. Alterations in FC between various regions are reported in Alzheimer's disease [69, 123], multiple sclerosis [18, 73] and schizophrenia [70, 124].

Resting state networks derived with the independent component analysis (ICA). ICA is a statistical approach that separates the fMRI signals into non-overlapping spatial and time components. It was initially introduced to identify and remove technical and physiological artefacts from the fMRI data, but ultimately helped to identify networks of FC in the human brain, so called resting state networks (RSN) [40, 99]. RSNs comprise of functionally connected regions during an unconstrained resting state that mimic networks involved in important brain operations like motor functions, visual processing, executive functioning, auditory processing, memory, attention and consciousness [26]. An example parcellation of the human cortex in seven resting state networks is depicted in Figure 6. Alterations in RSNs were associated with schizophrenia [76, 113], bipolar disorder [33] and were also found in pre-term born adults [6].

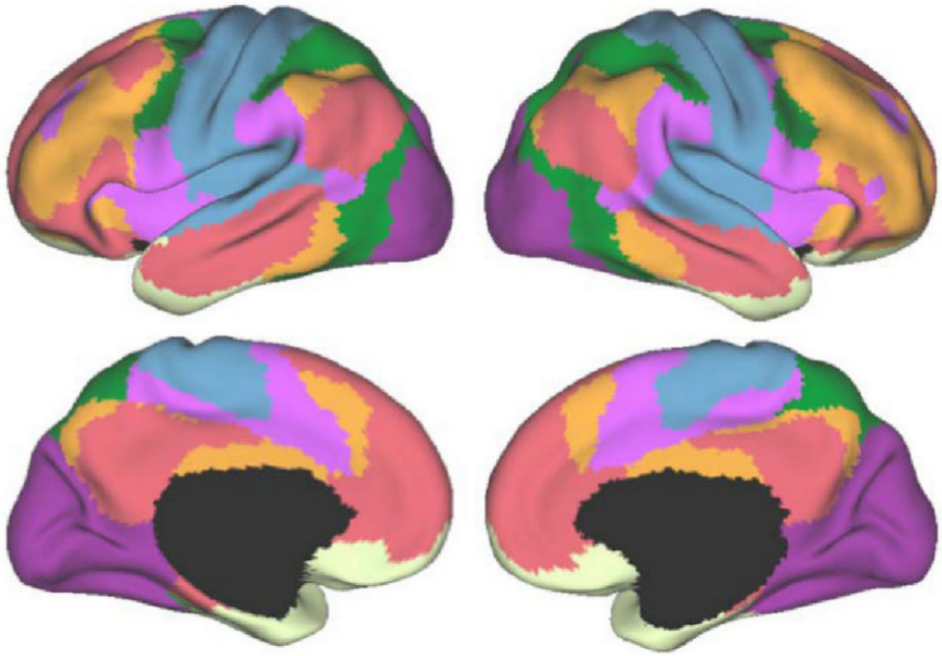

Figure 6: A parcellation of the human cerebral cortex in 7 resting-state networks as identified with ICA from rs-fMRI data (here a sample of 1000 healthy participants): visual (purple), somatomotor (blue), dorsal attention (green), ventral attention (violet), limbic (cream), frontoparietal (orange), default mode network (red). Adapted from [127]

6 Transcranial magnetic stimulation

TMS employs electromagnetic induction (of a 1–2.5 Tesla strenght) to depolarize cortical neurons. Generated by the TMS coil (placed tangentially towards the scull) short electromagnetic pulses pass through the scull inducing electric current in the tissue. The TMS produces trans-membrane ion flow in cortical axons that depolarizes the membrane potential and triggers an action potential (AP) in neurons. Activated neurons spread the AP to other brain areas [57]. The effects of TMS on the brain vary between regions because of differences in local tissue conductivity and electrical properties [43]. Transcranial magnetic stimulation is discussed as a therapeutic option to treat depression [100, 19], migraines [15] and patients that suffered stroke [52].

Part II

Aims and hypotheses

The aim of this dissertation is to investigate the role of the relationship between GABA and glutamate neurotransmitters and systems level brain activity in the visual system by combining MRS, fMRI and TMS.

Experiment 1 investigates fluctuations in MRS and fMRI signals in brain states of eyes closed (with no input), eyes open in darkness (with weak input) and visual stimulation (with strong visual input). GABA and Glx levels in the visual system were correlated with the BOLD signal change induced by visual input, and with measures of visual performance outside the scanner.

Experiment 2 examines the effects of non-invasive brain stimulation using TMS on MRS and BOLD signals in the visual system. Based on the network directionality model, parietal regions exert a top-down effect on visual cortex [101]. We therefore hypothesize that the TMS inhibition of top-down region would decrease the connectivity and affect neurotransmitter concentrations in the visual system.

Part III

Materials and methods

1 Participants and study design

After arriving at the experimental session, all volunteers were informed about the objectives and risks of the study and signed a written consent form. Participants were confirmed to not suffer from any neurodegenerative or psychiatric disorders and to not be under the influence of alcohol, drugs and medication (what could have altered MRS and fMRI scores). Both studies were approved by the local ethics committee. Detailed descriptions of study designs can be found in the following sections.

1.1 Experiment 1

Fifty-four healthy volunteers (M_{age}=27.3, SD=2.94, 29 males), divided in two cohorts, participated in experiment 1, which consisted of a neuroimaging and a behavioural session. The first cohort (24 volunteers) participated only in the neuroimaging part, and the second cohort (30 volunteers) took part in both: neuroimaging and behavioural session.

Scanning was performed on a 3T Biograph mMR integrated MR and PET system (Siemens, Erlangen, Germany) using vendor supplied 12-channel phase-array head coil. During the neuroimaging session, participants were placed in the scanner in a dimmed environment. After initial localizer and anatomical scans, counterbalanced sessions of MRS and fMRI sequences were acquired, including sessions of: eyes closed, eyes open and the visual stimulation (see Figure 7). Subjects were asked to lie down with their eyes closed without falling asleep, referred to here as the CLOSED condition, to keep

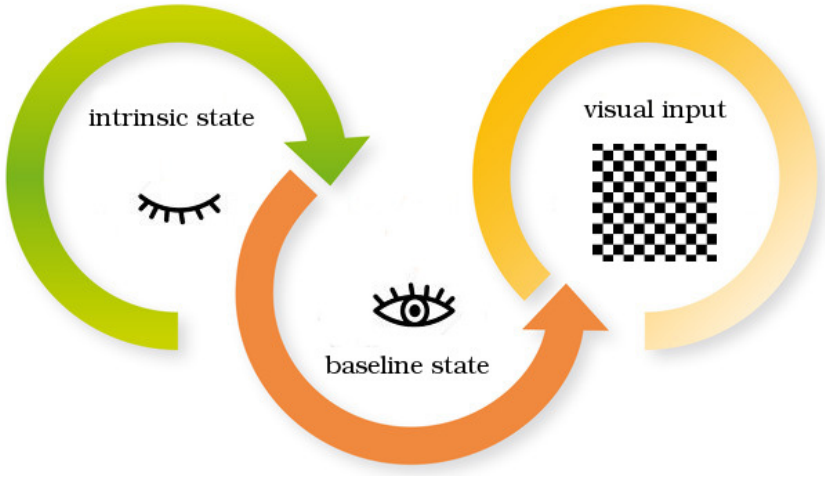

Figure 7: Scheme of MRS and fMRI experimental sessions in the Experiment 1.

their eyes open without receiving any visual input, i.e. the OPEN condition, and to look at a flickering chequerboard presentation (explained in details in section 2.2.1), the VIS STIM sessions. Participants from the first cohort performed only the CLOSED and OPEN conditions, whereas participants from the second cohort took part in all three conditions.

A few weeks after the initial neuroimaging experiment, volunteers from the second cohort performed two behavioural tasks described in section 2.4. Details of the neuroimaging pulse sequences used to acquire the data can be found in the sections 2.1.1 and 2.2.1.

1.2 Experiment 2

Thirty right-handed healthy volunteers took part in experiment 2 (M_{age}=25.9, SD=2.90, 16 females), each performing four counterbalanced sessions on four consecutive days; two comprised of MRS, and the other two of rs-fMRI measurements. In each session after the initial anatomical scan the following steps were performed:

- the baseline MRS or fMRI (pre-TMS) acquisition;

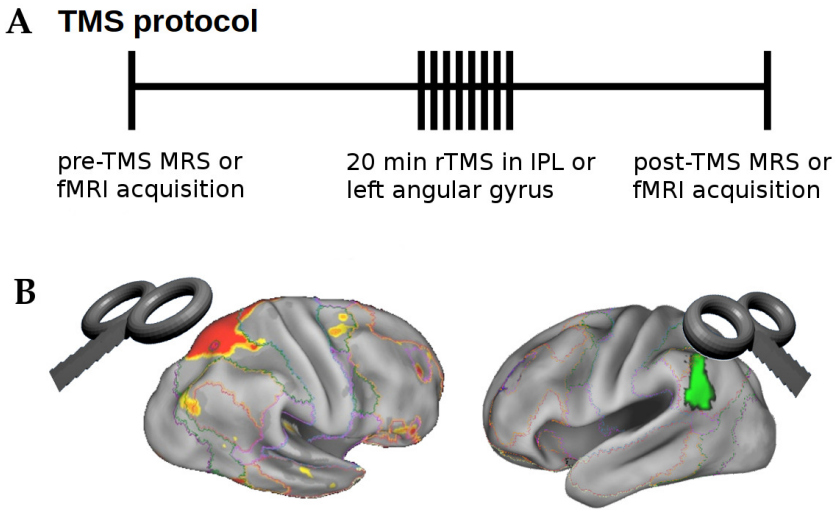

Figure 8: (A) Sequence of events in the Experiment 2. Initial MRS/fMRI acquisition was followed by the rTMS intervention, and later by the post-MRS/fMRI run. (B) Areas stimulated by the rTMS: left angular gyrus (left) and ipsolateral inferior parietal lobus (right).

- TMS stimulation;
- the post-TMS MRS or fMRI acquisition.

The experimental setup is depicted in Figure 8 A. Details of the TMS intervention session are described in section 2.3. The time between the end of the TMS stimulation and the start of the MRS or fMRI sessions was measured and kept as short as possible in order to enhance the rTMS effect.

During all acquisitions, participants were asked to stay awake with their eyes open, and to not fall asleep. This was ensured by observing their eyes with an MR-compatible camera (12M, MRC Systems, Heidelberg, Germany) installed on the coil. The scanner room was dimmed. Two areas were stimulated in separate TMS sessions: ipsolateral inferior parietal lobus (IPL) in the parietal cortex (as part of dorsal visual stream) and left angular gyrus (lAG) – a part of DMN network outside the visual stream (see Figure 8 B).

The post-TMS acquisitions were named post-TMS_{IPL} and post-TMS_{lAG}, respectively.

Neuroimaging data was acquired with 3 T Philips Ingenia scanner (Philips Healthcare, Best, The Netherlands) using the vendor-supplied 32-channel head coil. TMS stimulation was performed with the Nexstim eXimia NBS 4.3 system (Nexstim Oy, Helsinki, Finland). Details of the neuroimaging pulse sequences used to acquire the data can be found in sections 2.1.2 and 2.2.2. TMS stimulation protocol can be found in section 2.3.

2 Data acquisition

The neuroimaging data were acquired with Siemens and Philips scanners. Pulse sequence parameters specific for different vendors are described in details in the separate sections below.

2.1 Magnetic resonance spectroscopy

2.1.1 Siemens

MRS was acquired with the MEGA-PRESS pulse sequence provided by Siemens. For the first cohort WIP #715 was used and for the second cohort the updated version (WIP #795) was used respectively. A voxel with spatial resolution 25×25×25 mm^3 was centred within the visual cortex, in the midline, avoiding the scull proximity. The voxel placement is depicted in Figure 9. Both WIP sequences shared the following acquisition parameters: 256 single averages, bandwidth 1200 Hz, delta-frequency set to the position of creatine at -1.7 ppm relative to water. The following parameters were unique for the WIP #715 sequence: TR/TE=1500/68ms, vector size = 512, acquisition time 6 minutes and 30 seconds. Unique WIP #795 parameters included: TR/TE=2000/68 ms, vector

Figure 9: MRS voxel placement in the occipital cortex in the saggital and axial plane.

size 2048, acquisition time 8 minutes and 40 seconds.

2.1.2 Philips

GABA-edited MEGA-PRESS spectroscopy was acquired using the dedicated Philips pulse sequence developed and provided by Edden et. al. [37]. Two co-editing Gaussian pulses of a duration of 14 msec (bandwidth of FWHM inversion = 86.6 Hz) were applied at 1.9 ppm (ON scans) and 7.46 ppm (OFF scans). One hundred and sixty transients were acquired in 10 dynamic scans, each composed of a 16-scan cycle and containing 2048 data points. Spectral width was set to 2 kHz, TR/TE=2000/68ms. VAPOR water suppression was applied to the spectra; first and second-order shimming parameters were based on the pencil-beam projection-based shimming routine. Additional water-unsuppressed acquisition was run after each ON and OFF scan pairs and was later used for the tissue correction procedure. The total scan time was 10 minutes and 15 seconds.

2.2 Other magnetic resonance methods

2.2.1 Siemens

High resolution structural imaging. The magnetization prepared rapid acquisition gradient echo (MP-RAGE) T1-weighted anatomical image was acquired using following parameters: TR=2.3 ms, TE=2.98 ms, angle=9°, 160 covering the whole brain slices with gap=0.5 mm, FOV=256 mm, matrix size=256×256, voxel size=1.0×1.0×1.0 mm^3, and the total scan time of 5 minutes and 3 seconds.

fMRI. In the resting state fMRI paradigm, 360 volumes of EPI images (T2*-weighted echo-planar-imaging) in interleaved mode were acquired. Acquisition parameters were as following: TR=2 ms, TE=30 ms/angle, 90°, 35 slices aligned to AC/PC and covering the whole brain, FOV=192 mm, matrix size=64×64 voxels, voxel size 3.0×3.0×3.0 mm^3. Two counterbalanced blocks of CLOSED and OPEN conditions were acquired in 12 minutes and 6 seconds.

The visual stimulation paradigm shared the fMRI pulse sequence parameters with the resting state session and consisted of 10 interleaved blocks of task and rest, with a block length of 30 seconds. In total, 300 volumes were acquired in a scan time of 10 minutes and 6 seconds. Detailed description of the presentation used in the visual stimulation paradigm is described in the the following paragraph.

Visual stimulation paradigm. In the VIS STIM condition, a black-white flickering chequerboard was presented with frequency of 8 Hz. Ten interleaved 30-second blocks of signal ON and rest (a black fixation cross on the white background) were presented. Participants were asked before the experiment to pay attention to the stimuli when the chequerboard was flickering, and to fixate on the cross during the rest block. Stimula-

tion was presented on BOLD Screen 32 MR Safe Display (Cambridge Research Systems, Cambridge, UK) with a resolution of 1920x1080 and a frame rate of 120 Hz. The screen was placed in the back of the scanner's bore. Participants viewed the presentation on a mirror installed on the coil.

2.2.2 Philips

High resolution structural imaging. The T1-weighted 3D-TFE anatomical image was acquired using the following parameters: TR=9 ms, TE=3.98 ms, angle=8°, 170 slices with gap=1 mm, covering the whole brain, FOV=256 mm, matrix size=256×256, voxel size=0.7×0.7×0.7 mm^3, and a total scan of time 5 minutes and 58 seconds.

fMRI. Multiband EPI sequence with blipped-controlled aliasing was used to acquire the resting state fMRI data [94] with the following parameters: voxel size 3×3×3 mm^3, multiband factor of 2, SENSE factor of 2, TR=1.25 seconds, TE=30 ms, flip angle of 90°, 40 slices covering the whole brain. In total, 600 volumes were acquired in 12 minutes and 35 seconds.

2.3 Transcranial magnetic stimulation

TMS intervention was performed by applying inhibitory, low-frequency (1 Hz) repetitive navigated TMS (rTMS) to the lAG and IPL, see Figure 8. Before the first experimental session, the individual's resting state motor threshold (rMT) was assessed. The MT area was derived from the hand knob corresponding to the cortical representation of the abductor pollicis brevis muscle (APB). The rTMS stimulation intensity in later sessions was set to individual's rMT intensity.

In 20 minutes of rTMS intervention 1200 pulses were applied on the target area. During

Participant	rMT threshold	Participant	rMT threshold	Participant	rMT threshold
1	31%	11	45%	21	48%
2	35%	12	29%	22	48%
3	27%	13	32%	23	29%
4	33%	14	30%	24	36%
5	30%	15	43%	25	31%
6	36%	16	27%	26	35%
7	31%	17	35%	27	35%
8	35%	18	30%	28	28%
9	27%	19	57%	29	34%
10	31%	20	34%	30	30%

Table 1: Individual resting state motor threshold (rMT) assessed before the first TMS session in the Experiment 2.

the stimulation, the coil was angulated perpendicular to the skull surface, and anterior-posterior orientation of the induced electric field was maintained throughout using an adjustable coil holder.

2.4 Behavioural experiments

Subjects who took part in the neuroimaging session of Experiment 1 performed two visual experiments: an orientation discrimination task and an attentional capture task as a control task (organized in the counterbalanced order). The orientation discrimination task employs basic visual processes depending on excitatory-inhibitory neurotransmission balance in the visual system [8, 20, 36]. In contrast, the attentional capture search engages

high-level attentional resources and strongly depends on saliency processes.

The experimental protocols were approved by the ethical review board of the Faculty of Psychology and Education of the Ludwig-Maximilians-Universität München and performed in the Department of Experimental Psychology of the LMU. Throughout the testing, participants were required to have normal or corrected-to-normal vision.

2.4.1 Orientation discrimination experiment

Apparatus. Gaze position was recorded using an EyeLink 1000 Desktop Mount (SR Research, Osgoode, Ontario, Canada) at a sampling rate of 1 kHz. Participants' head movements were minimized using a chin and forehead rest. The experiment was controlled by an Apple iMac Intel Core i5 computer (Cupertino, CA, USA) and the experimental software was implemented in Matlab (MathWorks, Natick, MA, USA), using the Psychophysics [16, 92] and EyeLink toolboxes [59]. Stimuli were presented at a viewing distance of 60 cm on a 21-in gamma-linearized SONY GDM-F500R CRT screen (Tokyo, Japan) with a spatial resolution of 1024x768 pixels and a vertical refresh rate of 120 Hz.

Procedure. The orientation discrimination design was adopted and modified from Edden, 2009 [36]. Subjects initially fixated at a central black fixation dot (0 cd/m^2, 0.15° radius), on a gray background (30 cd/m^2), see Figure 10. Once a stable fixation was detected within a 2.0° radius virtual circle centred on the fixation dot, a flickering Gabor/Noise-stream appeared at the fixation. The stimulus was composed of interleaved sequences of vertically oriented Gabor patches (frequency 2.5 cpd, random phase, 100% contrast, standard deviation of Gaussian envelope 1.1°, mean luminance 30 cd/m^2) and Gaussian pixel noise patches (0.22°-width pixels ranging from white (1) to black (0), same Gaussian envelope as for the Gabors), alternating every 25 ms. After 400–800 ms, this stream com-

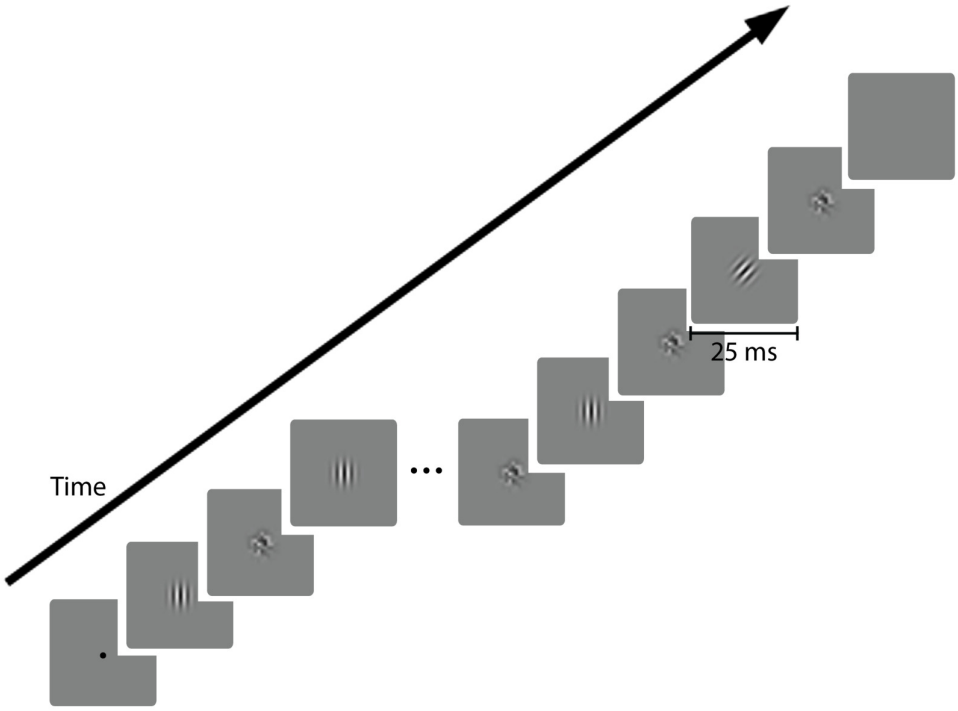

Figure 10: Orientation discrimination task. Sequence of events in the course of each trial.

prised a discrimination Gabor patch was slightly rotated clockwise or counter-clockwise. Following the method of constant stimuli, tilt angles (nine linearly spaced angles from 1° to 17°) varied randomly across trials. After 25 ms, the oriented Gabor patch was masked by another noise patch. 200 ms afterwards, the Gabor/Noise-stream disappeared and participants indicated via button press in a non-speeded manner whether the discrimination Gabor was tilted clockwise or counter-clockwise. They received a negative feedback sound for incorrect responses. After one practice block, each participant performed seven blocks of 35 trials. We controlled online for broken fixation (not within 2.0° from FT) and repeated erroneous trials in random order at the end of each block.

2.4.2 Attentional capture experiment

Stimuli and Design. The attentional capture paradigm, adapted from Theeuwees, 1992 [116], was implemented in the Open Sesame software (version 3.1.6b1 [78]), modified

and ran on an Intel computer. The visual display comprised of 8 circular (1.4° in diameter) or rectangular geometric stimuli (100 px). Yellow (97.6 cd/m^2) and blue (12.3 cd/m^2) shapes were displayed on the black background (1.24 cd/m^2). In each trial, one of the stimuli was in a unique shape (e.g. seven circular, one rectangular). The target, a white line segment (111 cd/m^2, 75 px), was presented inside of unique shape in either a vertical or a horizontal orientation (with possible options: 0° or 90°), see Figure 11 A. Other line segments inside geometric figures were tilted either to the right or to the left (possible orientations: 30°, 60°, 120°, 150°), and distributed randomly on the display. In distractor absent trials, all shapes were presented in the same color (for example: seven circular shapes and one rectangular shape, all blue). In distractor present trials, one of the blue circles was replaced with a yellow circle (see Figure 11 B). Participants were asked to indicate the orientation of the line segment in the unique shape. The experiment consisted of 7 blocks 20 trials each (140 trials in total). Chin rest was used to stabilize the observer's head at a 55 cm distance from the screen with a visual angle of 0.7°x0.7°.

Procedure. After receiving written and oral instructions about the experimental procedure, the experiment was started with a block of practice session (20 trials). The goal of the practice was to familiarize participants with the task. Next, the remaining six blocks of experiment were performed.

In the beginning of each trial, a black fixation dot at the center of the screen was presented for 500 ms. The stimuli display was presented subsequently and remained on the display for 300 ms. Subjects were instructed to respond as fast and as accurate as possible, and to indicate the orientation of the line in the unique shape as vertical or horizontal. After an erroneous response, a red dot was presented on the location of the fixation dot for 500 ms. The inter-trial interval was 500 ms.

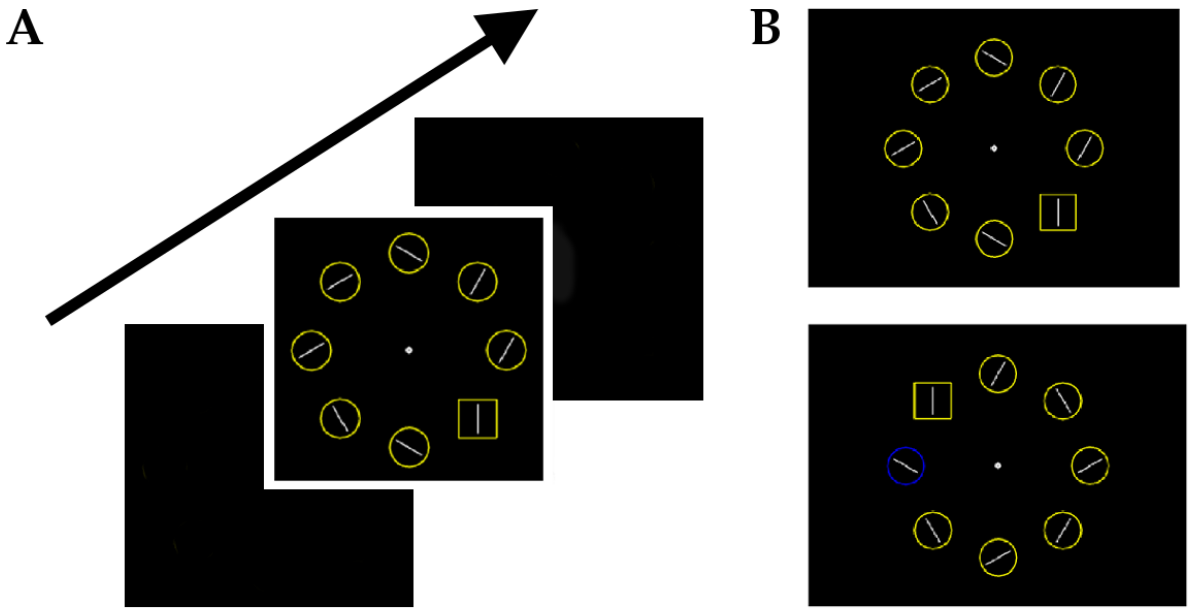

Figure 11: Attentional capture task. (A) Sequence of events in the course of each trial. (B) Illustration of the example stimuli presentations as distractor absent (upper panel) and distractor present (lower panel).

3 Data analysis

3.1 Magnetic resonance spectroscopy

The MEGA-PRESS spectra were exported from the scanner in the .rda (Siemens) or .sdat (Philips) format and analysed with the Gannet 2.0 software [37]. Preprocessing steps included: time-domain correction, frequency and phase correction, filtering with 3 Hz, line broadening and fitting choline and creatine signals. After subtracting OFF from ON acquisitions, the single GABA+[1] peak at 3 ppm and the double Glx[2] peak at 3.75 ppm were separately fitted using a five-parameter Gaussian model, and referenced to Cr signal. Example GABA and Glx fits are shown in Figure 12 A and B.

Averaged group GABA and Glx peak full width at half maximum (FWHM) were analysed and compared between conditions in order to control for blood flow effects [12]. The relationship between GABA/Cr and Glx/Cr concentrations were assessed with the Pearson product-moment correlation coefficients. Shapiro tests assuring the normality of the distribution were performed.

The "edit-off" spectra were analysed with LCModel version 6.3-1 [96]. With the simulated basis set provided by the software developer, ratios of Asp, GSH, Ins, PCh and NAA to creatine were calculated. The spectra with peak fitting errors (Cramer-Rao minimum variance bounds) exceeding 20% were removed from further analysis. Example fits are shown in Figure 12 C.

In order to extract the fMRI scores from the voxel of interest corresponding to the individually placed MRS voxel, a voxel coregistration procedure was performed with the Gannet 2.0 software [37].

[1] GABA+: GABA peak with a contribution from macromolecule signals

[2] Glx: combined Glu and Gln signals mainly derived from Glu

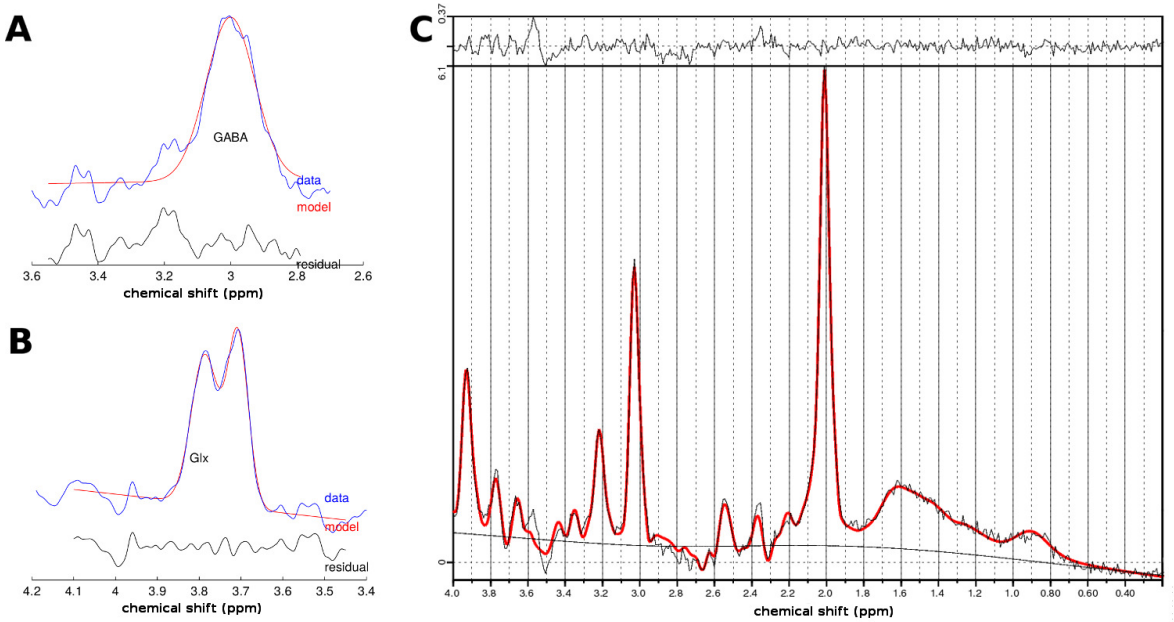

Figure 12: Sample fits of edited and "edit-off" spectra. A) GABA fit in the edited spectrum; B) Glx fit in the edited spectrum; C) LCModel fit of the "edit-off" spectrum.

3.1.1 Siemens

Following the preprocessing and peak fitting, the quality control of all the acquisitions was performed. From the total of 146 runs, either GABA or Glx could not be fitted in three runs and were therefore excluded. Later, we excluded any run that exceeded 3 SD from the group mean in any of the following parameters: GABA, Glx or Cr fit error, GABA FWHM, and Glx FWHM, which led to an exclusion of further 3 runs. Plots depicting quality check parameters of all acquisitions can be found in Figure 13.

The effects of brain states on metabolites concentrations in edited and "edit-off" signals were assessed in CLOSED, OPEN and VIS STIM conditions with ANOVAs and two-tailed paired-samples t-tests. Individual data were used for the integrative MRS-fMRI analysis.

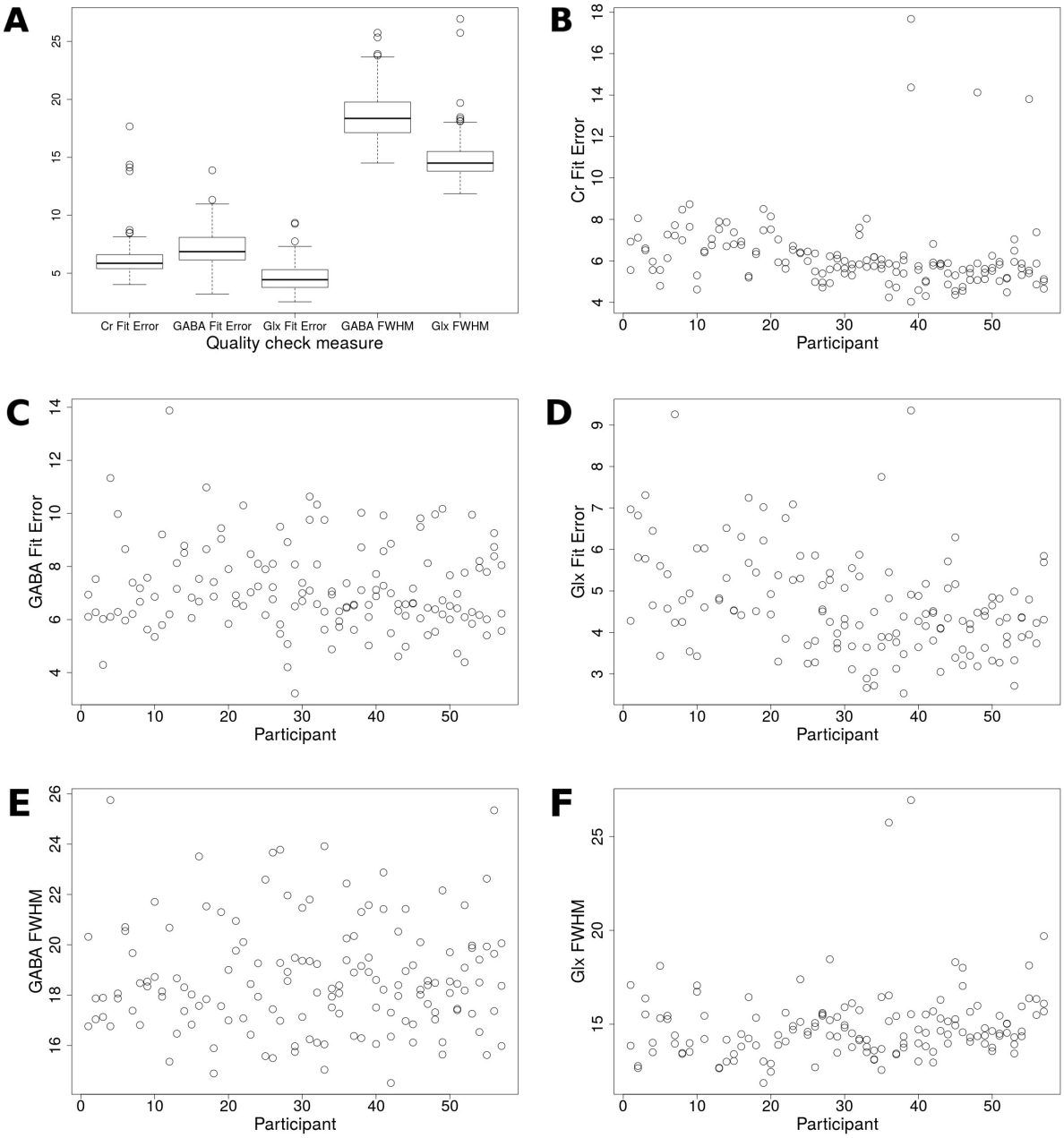

Figure 13: Plots depicting single subjects' parameters used to assess the quality of spectroscopy data in Experiment 1. A) Boxplots representing all parameters of interest; B) scatterplot representing Cr fit error values; C) scatterplot representing GABA fit error values; D) scatterplot representing Glx fit error values; E) scatterplot representing GABA peak full width at half maximum (FWHM); F) scatterplot representing Glx peak full width at half maximum (FWHM).

3.1.2 Philips

From 120 separate MRS runs, all the spectra were fitted successfully. After inspecting the data quality parameters (GABA, Glx and Cr fit error, GABA FWHM, and Glx FWHM), three acquisitions were excluded due to the score exceeding 3 SD of the whole group. Plots depicting quality check parameters of all acquisitions can be found in Figure 14.

Based on recent reports, referencing GABA to water peak (GABA/H_2O) instead of creatine (GABA/Cr) quantifies GABA concentrations in the MRS voxel more accurately [50] as it allows the correction for voxel composition of gray matter, white matter and cerebrospinal fluid. Thanks to additionally acquired water-unsuppressed scan in the MEGA-PRESS sequence on Philips scanner, we analysed the GABA/H_2O in addition to the GABA/Cr signals. Four GABA/H_2O fits were missing due to a lack of unsuppressed water file.

The effects of TMS intervention on metabolites concentrations in edited and "edit-off" signals were assessed in pre-TMS (average between the pre-TMS_{AG} and pre-TMS_{PAR} sessions), post-TMS_{AG}, and post-TMS_{PAR} conditions with ANOVAs and post-hoc two-tailed paired-samples t-tests and corrected for multiple comparisons with the Bonniferroni correction. Individual data were used for the integrative MRS-fMRI analysis.

3.2 fMRI

The preprocessing of fMRI data was performed with DPARSF tool and SPM8 functions, all implemented in Matlab (Wellcome Trust Center for Neuroimaging, University College London, www.fil.ion.ucl.ac.uk/spm) [21, 107]. The preprocessing included following steps: slice timing, realignment and reorientation. None of the subjects exhibited 3 mm of maximal rotation and 3 degrees of maximal translation of overall estimated head motion

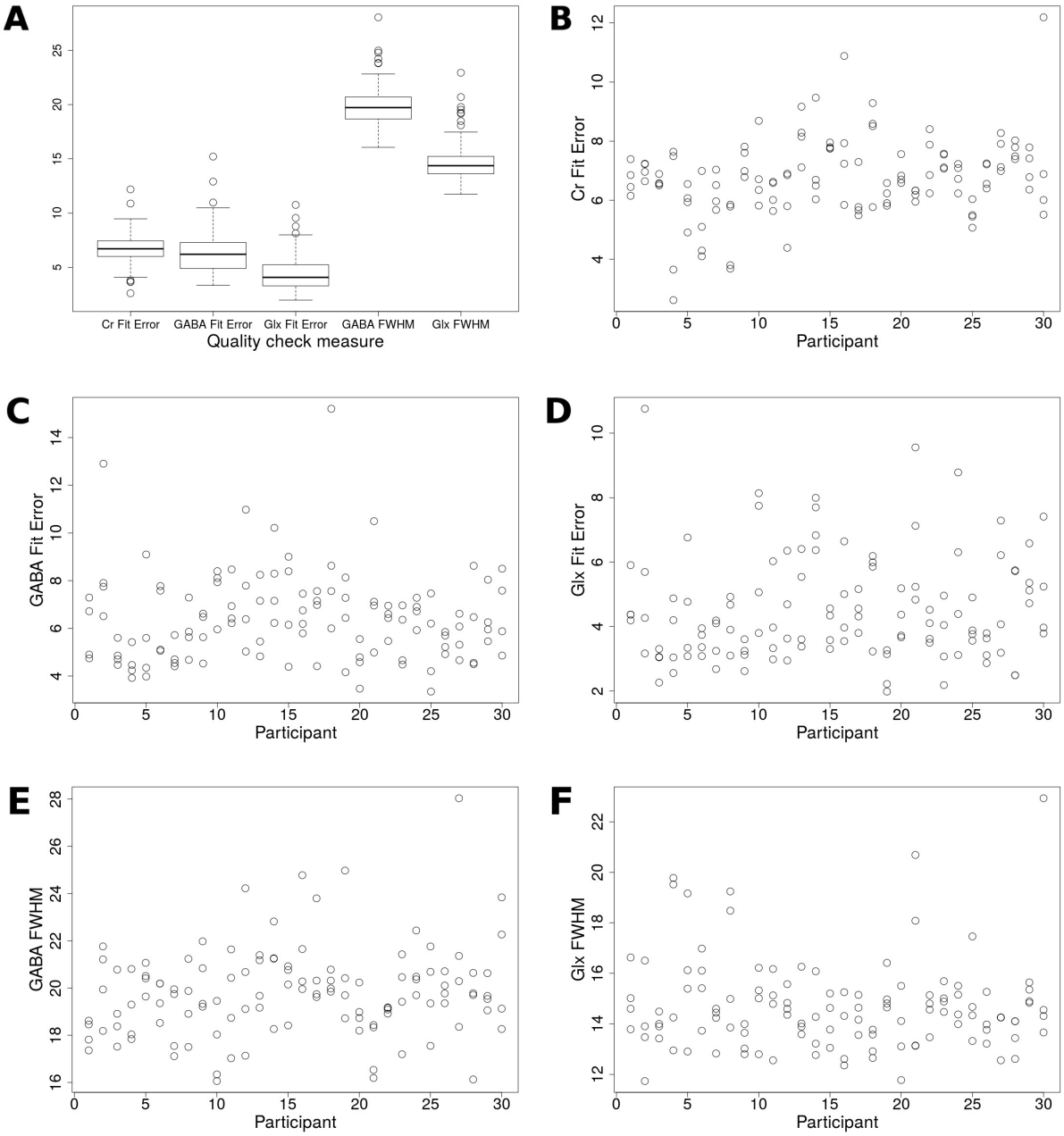

Figure 14: Plots depicting single subjects' parameters used to assess the quality of spectroscopy data in Experiment 2. A) Boxplots representing all parameters of interest; B) scatterplot representing Cr fit error values; C) scatterplot representing GABA fit error values; D) scatterplot representing Glx fit error values; E) scatterplot representing GABA peak full width at half maximum (FWHM); F) scatterplot representing Glx peak full width at half maximum (FWHM).

during the course of the experiment. After the coregistration of structural image to the functional mean volume, the structural volume was segmented, and the mean white matter and CSF signals were regressed out from the functional signal.

The rs-fMRI data analysis to derive probabilistic Independent Component Analysis (pICA) scores [9] was performed with FEAT (FMRI Expert Analysis Tool) Version 6.00 and MELODIC (Multivariate Exploratory Linear Decomposition into Independent Components) Version 3.14, both being part of the FSL software package (FMRIB's Software Library).

Amplitude of low frequency fluctuations (ALFF). The preprocessed fMRI data were smoothed with 4 mm Gaussian kernel, detrended, and kept in the subjects' native space without normalization. The signal time series from each voxel in the frequency range of 0.01-0.1 Hz were transformed into the frequency domain. The square root of each frequency was calculated and averaged [129]. Standardized Z-score ALFF maps were used for the later analysis. The zALFF scores from voxels of interest corresponding to the individually placed MRS voxel were extracted and averaged with Matlab. Difference between CLOSED and OPEN conditions was assessed with a two-tailed paired-sample t-test; individual zALFF scores were used for the integrative MRS-fMRI analysis.

Functional connectivity (FC). The preprocessed data were smoothed with 4 mm Gaussian kernel, detrended and filtered with bandpass filter of 0.01-0.1 Hz. Next, the seed-based FC was calculated between the ROI corresponding to the MRS voxel and the visual resting state network (derived from the 7-networks parcellation [127]). Functional connectivity maps were normalized and transformed into Z-score maps. zFC scores from the voxel of interest corresponding to the individually placed MRS voxel were extracted

and averaged with Matlab. Eventually, group difference between CLOSED and OPEN conditions was assessed and individual scores were used for the integrative MRS-fMRI analysis.

BOLD signal change. This section describes the analysis of BOLD signal change during task conditions. After preprocessing, the structural and functional images were coregistered, normalized to MNI space and smoothed using a 6 mm FWHM Gaussian kernel. To analyze statistical differences between blocks of task and rest conditions, 10 interleaved blocks of ON and OFF were modelled with the SPM canonical haemodynamic response function with motion parameters added to the general linear model. To account for the multiple regression comparisons, a family-wise error correction was used ($p<0.05$, corrected) for the mass-univariate voxel-wise testing. The contrast of interest was defined as ($beta_{visual}$ – $beta_{rest}$). The contrast estimates were extracted from the individuals' peak voxels located in the visual cortex and were used for later analysis. At this stage, one participant had to be excluded, because of no significant activation cluster (FWE-corrected) in the visual cortex.

Independent component analysis (ICA). Data preprocessing for the ICA analysis included motion correction using MCFLIRT (motion correction FLIRT), removal of non-brain tissues with BET (brain extraction tool), spatial smoothing with 6 mm Gaussian kernel, intensity normalization and high-pass temporal filtering. Functional data were registered to the structural volume and normalized to the MNI space. Next, using the MELODIC algorithm, datasets of all subjects were temporally concatenated, whitened and projected into 25 dimensional components using Principal Component Analysis. The dual regression was run on the set of spatial maps created in the previous step, in which

subject-specific spatial maps were generated and associated with time series [10].

First step of dual regression was to regress out the group-average set of spatial maps from the single subject's 4D data set. The time series from the previous step were then regressed out as temporal regressors from the same 4D data sets. As a result, subject-specific spatial maps were created, one per group-level spatial map. At last, visual and dorsal attentional network components were selected by visual inspection and used for further analysis as they reflect parts of the visual processing stream. ICA scores from the voxel of interest corresponding to the individually placed MRS voxel were extracted and averaged with Matlab. The difference between CLOSED and OPEN conditions was assessed with two-tailed paired-sample t-test. Individual ICA scores were used for the integrative MRS-fMRI analysis.

3.3 Behavioural experiments

3.3.1 Orientation discrimination

By fitting cumulative Gaussian functions to each subject's performance, the tilt angle corresponding to 75% correct performance in orientation discrimination was determined. Five participants were not able to discriminate any of the tilt angles above chance level (50% correct), and therefore were excluded from further analysis.

3.3.2 Attentional capture

After excluding error trials from the analysis, the mean and the accuracy of distractor absent and distractor present trials were analysed. A paired-sample one-tailed t-test was used to assess the difference between the conditions of distractor absent and distractor present. Regression analysis was used to assess the relationship between the concentration

of metabolites, fMRI scores and behavioural results.

3.4 Statistical analysis

In experiments 1 and 2, the differences in metabolites' concentrations at the group level between conditions were assessed by one-way between subjects ANOVAs and post-hoc paired-sample two-tailed t-tests (corrected for multiple comparisons with the Bonferroni correction). Shapiro tests were run to assure normal distribution of the data. The effect of GABA and Glx line broadening when comparing conditions was controlled by analysing the FWHM of neurotransmitters peaks with one-way between subjects ANOVAs. Concentrations of GABA+/Cr and Glx/Cr were correlated using Pearson Correlation Coefficient method. GABA+/Cr, GABA/H_2O and Glx/Cr concentrations in the voxel of interest were correlated with fMRI measures and behavioural scores using using Pearson Correlation Coefficient method. Statistical and behavioural data analyses were performed with the "R" package [24].

Part IV

Results

1 Experiment 1. The role of GABA and Glx in the visual system

1.1 GABA and Glx concentration in different brain states

We performed the analyses of neurotransmitter concentrations in the CLOSED and OPEN conditions on the concatenated data from both cohorts. In addition, we used the second cohort to assess the differences between the CLOSED, OPEN and VIS STIM conditions.

GABA. A two tailed t-test revealed a significant decrease in GABA concentration ($t(47)=3.78$, $p=0.0004$) from CLOSED ($M=0.115$, $SD=0.0154$) to OPEN ($M=0.106$, $SD=0.0121$) condition, see Figure 15 A and B, and Table 2. For the second cohort, a one-way between subjects ANOVA revealed a significant main effect of brain state on GABA concentrations in CLOSED, OPEN, and VIS STIM conditions ($F(2, 82)=5.49$, $p=0.006$). Post-hoc paired-sample two-tailed t-tests again revealed decrease in GABA concentrations ($t(25)=3.39$, $p=0.00693$, corrected for multiple comparisons) from CLOSED ($M=0.115$, $SD=0.0162$) to OPEN ($M=0.103$, $SD=0.0117$) conditions, but neither the difference between CLOSED and VIS STIM ($p>0.08$) nor between OPEN and VIS STIM ($p>0.22$) was significant, see Figure 16 A and B, and Table 2. In summary, GABA concentration dropped from the CLOSED to OPEN state with no further change during the processing of visual input in the VIS STIM condition.

GABA+/Cr concentration			
Group	CLOSED (SD)	OPEN (SD)	STIM (SD)
Cohort II (n=31)	0.115 (0.0162)	0.103 (0.0117)	0.107 (0.0121)
Both cohorts (n=54)	0.115 (0.0154)	0.106 (0.0121)	—
Glx/Cr concentration			
Group	CLOSED (SD)	OPEN (SD)	STIM (SD)
Cohort II (n=31)	0.101 (0.0096)	0.106 (0.0114)	0.110 (0.0105)
Both cohorts (n=54)	0.094 (0.0130)	0.096 (0.0150)	—

Table 2: Group averaged GABA+/Cr and Glx/Cr concentrations in the CLOSED, OPEN and VIS STIM conditions derived from edited MEGA-PRESS acquisition and analysed with gannet. Standard deviation values are given in brackets.

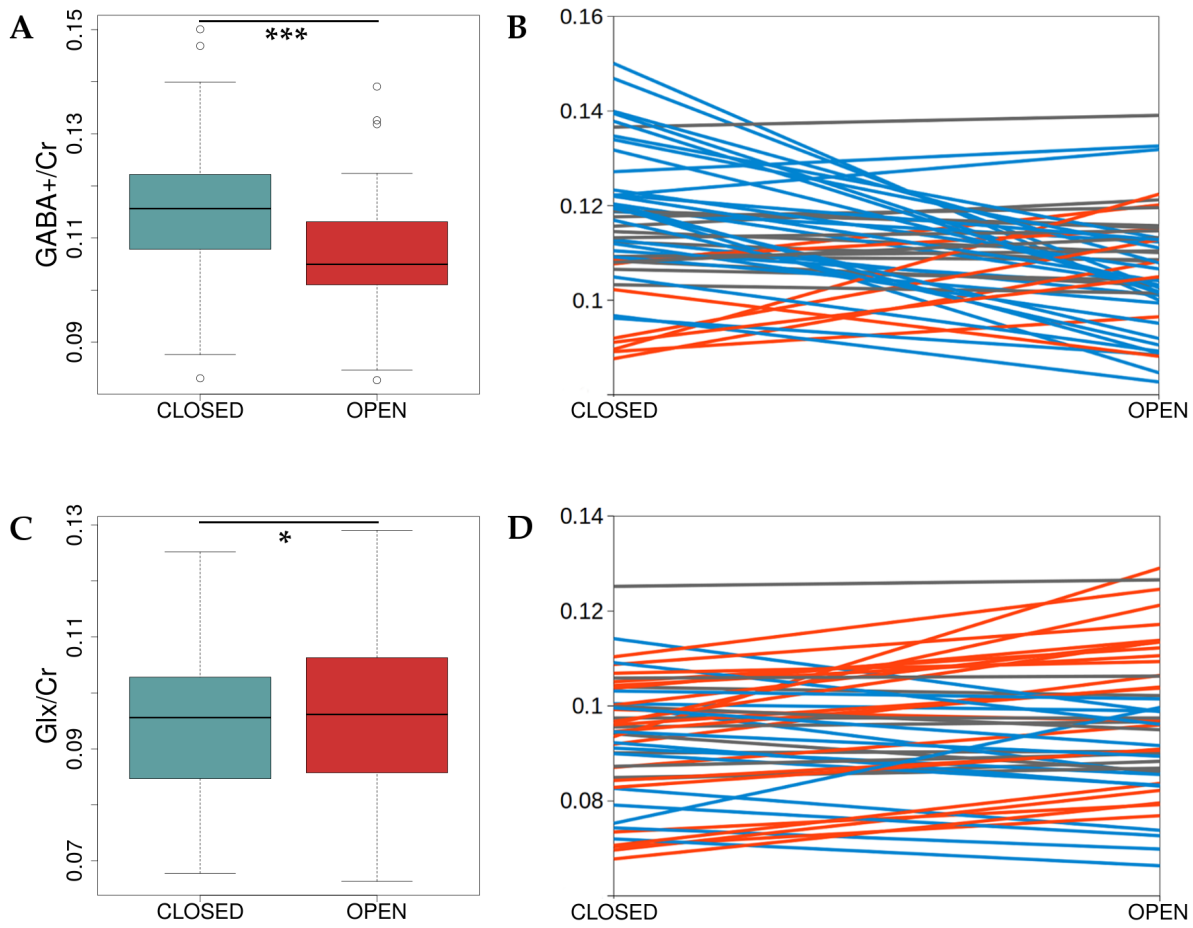

*Figure 15: Concentrations of metabolites in the visual cortex in CLOSED and OPEN conditions: data concatenated from both cohorts. (A,C) Box plot of group GABA+/Cr and Glx/Cr concentrations. Statistically significant differences are marked with * ($p<0.05$), and *** ($p<0.001$). (B,D) Changes of GABA+/Cr and Glx/Cr in individual subjects; red line depicts $\geqslant 5\%$ concentration increase between conditions, blue line: $\geqslant 5\%$ decrease; if the concentration change was $\leqslant 5\%$, a gray line was drawn.*

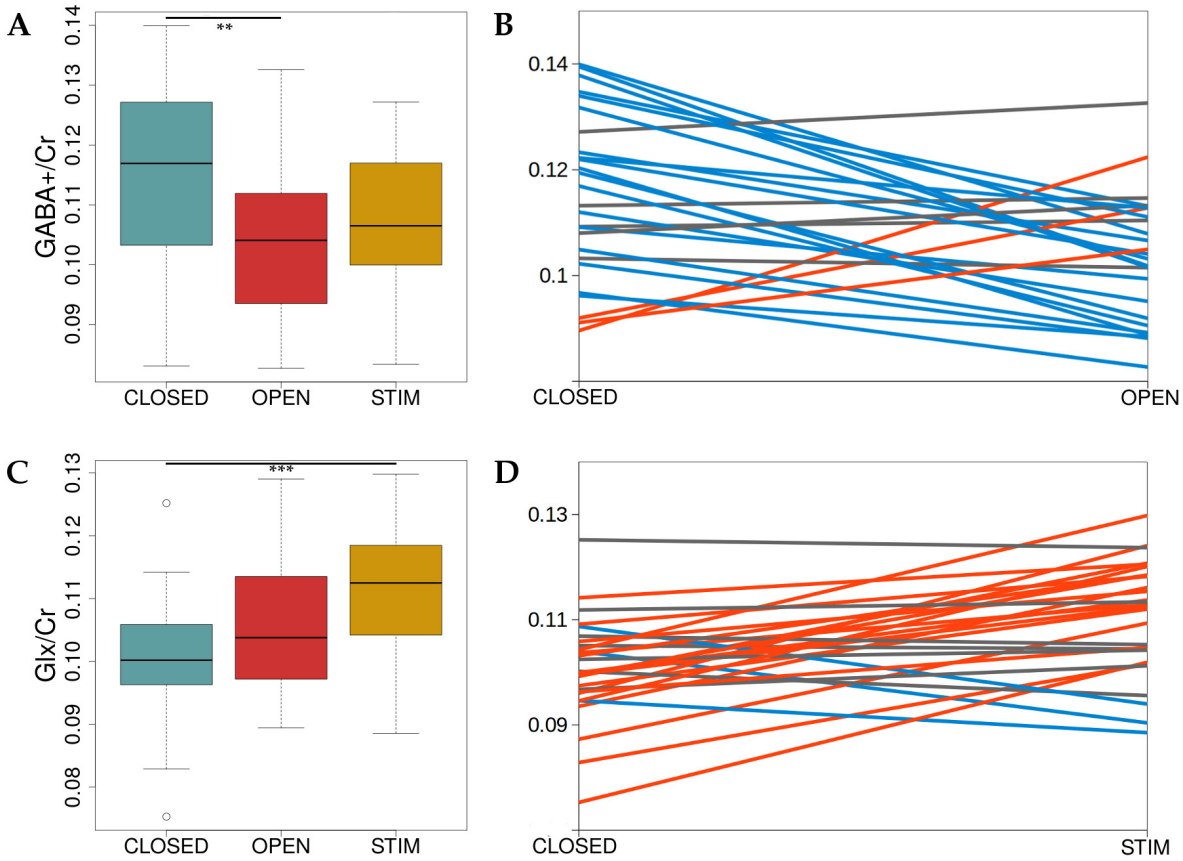

*Figure 16: Concentrations of metabolites in the visual cortex in CLOSED, OPEN, and VIS STIM conditions. (A,C) Box plot of group GABA+/Cr and Glx/Cr concentrations. Statistically significant differences are marked with ** ($p<0.01$) and *** ($p<0.001$). (B,D) Changes of GABA+/Cr and Glx/Cr in individual subjects; red line depicts $\geqslant 5\%$ concentration increase between conditions, blue line: $\geqslant 5\%$ decrease; if the concentration change was $\leqslant 5\%$, a gray line was drawn.*

Glx. A two tailed t-test revealed a significant increase in Glx concentration (t(47)=-2.17, p=0.035) from CLOSED (M=0.094, SD=0.0130) to OPEN (M=0.096, SD=0.0150) condition, see Figure 15 C and D, and Table 2. For the second cohort, a one-way between subjects ANOVA revealed a significant main effect of brain state on Glx concentrations in CLOSED, OPEN, and VIS STIM conditions (F(2, 82)=4.59, p=0.013). Post-hoc paired-sample two-tailed t-tests again revealed an increase in Glx concentrations from CLOSED (M=0.101, SD=0.0096) to VIS STIM (M=0.106, SD=0.0114) conditions (t(27)=4.27, p=0.00642, corrected for multiple comparisons), with an average increase of 10.44%, but no difference between OPEN and STIM conditions (t(25)=1.61, p=0.1196), see Figure 16 C and D, and Table 2. There was a marginally significant Glx concentration increase from CLOSED to OPEN (M=0.106, SD=0.0114) conditions (t(27)=4.27, p=0.00642) with an average signal change of 3.91%. In summary, Glx concentration did not differ between the two baseline states of eyes CLOSED and OPEN (in darkness) but increased with visual input.

In addition, we performed control analyses to verify the stability of GABA and Glx peak widths and the normality of the distribution between brain states. We also assessed whether direct correlations exist between both neurotransmitters across subjects which would question the independence of the two signals from the MRS spectrum.

GABA and Glx peak width. A one-way between subjects ANOVA was conducted to compare the effect of linewidth (FWHM) changes in GABA and Glx spectra in CLOSED, OPEN and VIS STIM conditions. There was no significant effect of linewidth change neither in GABA (F(2, 88)=0.89, p=0.41) nor in Glx (F(2, 88)=0.97, p=0.38) for the three conditions at the $p<0.05$ level, see Table 3.

GABA FWHM			
Group	CLOSED (SD)	OPEN (SD)	STIM (SD)
Cohort II (n=31)	18.82 (2.506)	18.26 (2.216)	19.01 (2.009)
Both cohorts (n=54)	18.84 (2.264)	18.17 (1.909)	—
Glx FWHM			
Group	CLOSED (SD)	OPEN (SD)	STIM (SD)
Cohort II (n=31)	15.19 (2.365)	14.59 (1.116)	15.02 (1.332)
Both cohorts (n=54)	14.91 (2.112)	14.51 (1.191)	—

Table 3: Group averaged FWHM scores of GABA and Glx peaks in CLOSED, OPEN and VIS STIM conditions. Standard deviation values are given in brackets.

Normality of group results distribution. GABA and Glx group results in three conditions were tested for violation of normality of distribution with the Shapiro-Wilk test ($p<0.05$). All group values were distributed normally. Group W-scores and p-values can be found in Table 4.

Correlation between GABA and Glx. Pearson product-moment correlation coefficients were computed to assess the relationships between GABA and Glx values in each of three conditions. There were no significant correlations between the variables; r- and p-values can be found in Table 5.

To summarize, the control analyses revealed no changes in GABA and Glx linewidth stability and the normality of the distribution between conditions. There was also no significant correlation found between the neurotransmitter concentrations across conditions.

Shapiro test results for GABA+/Cr group averages: W-scores and p-values			
Group	CLOSED	OPEN	STIM
Cohort II (n=31)	0.9691, p=0.51	0.9690, p=0.51	0.9687, p=0.61
Both cohorts (n=54)	0.9821, p=0.62	0.9777, p=0.43	—
Shapiro test results for Glx/Cr group averages: W-scores and p-values			
Group	CLOSED	OPEN	STIM
Cohort II (n=31)	0.9603, p=0.28	0.9556, p=0.26	0.9740, p=0.62
Both cohorts (n=54)	0.9714, p=0.22	0.9889, p=0.83	—

Table 4: Shapiro test results of GABA+/Cr and Glx/Cr in the CLOSED, OPEN and VIS STIM conditions. W-scores and p-values are depicted for each separate group of interest.

Pearson correlation coefficients and p-values			
Group	CLOSED	OPEN	STIM
Cohort II (n=31)	-0.242 (p=0.21)	-0.218 (p=0.26)	-0.058 (p=0.76)
Both cohorts (n=54)	-0.078 (p=0.59)	-0.199 (p=0.16)	—

Table 5: Correlation coefficients between GABA+/Cr and Glx/Cr in the CLOSED, OPEN and VIS STIM conditions; p-values are given in brackets.

Metabolites concentration in the "edit-off" spectrum.				
Metabolite	CLOSED (SD)	OPEN (SD)	STIM (SD)	ANOVA F(2,81)
Asp	0.28 (0.060)	0.29 (0.051)	0.28 (0.053)	F=0.97, p=0.38
GSH	0.20 (0.019)	0.20 (0.020)	0.20 (0.017)	F=0.45, p=0.64
Ins	0.76 (0.076)	0.76 (0.078)	0.73 (0.069)	F=0.09, p=0.92
GPC+PCh	0.15 (0.013)	0.15 (0.014)	0.14 (0.011)	F=0.03, p=0.98
NAA+NAAG	1.68 (0.101)	1.68 (0.099)	1.71 (0.086)	F=0.04, p=0.96

Table 6: Group averaged metabolites concentrations in the "edit-off" spectrum in the CLOSED, OPEN and STIM conditions. Standard deviation values are given in brackets. A one-way between subjects ANOVA scores comparing metabolite concentrations in three conditions are shown in the last column.

1.2 Concentration of other metabolites in different brain states

Here, we tested for the specificity of state changes on GABA- and Glx-levels and therefore assessed the effect of different states on the concentrations of other metabolites in the same spectrum. One-way between subjects ANOVAs were conducted to compare the effect of brain state on Asp, GSH, Ins, PCh and NAA concentrations in CLOSED, OPEN, and VIS STIM conditions. There was no significant effect of condition on those metabolites at the $p<0.05$ level, which suggests that the changes in brain states only affected the inhibitory and excitatory neurotransmitters and not other metabolites. Group averaged metabolite concentrations can be found in Table 6.

1.3 fMRI measures in different brain states

Using rs-fMRI data from CLOSED and OPEN conditions, we analysed neural activity on the local level within the MRS voxel (measured with the ALFF) and across the visual system (measured with seed-based FC).

ALFF in the visual cortex. A paired-sample two-tailed t-test was conducted to compare zALFF score differences in CLOSED (M=0.69, SD=0.556) and OPEN (M=0.77, SD=0.384) conditions. There was no significant difference in zALFF scores (t(53)=1.01, p=0.31) between conditions. Box plot and one sample t-test map of zALFF scores can be found in Figure 18 A and B.

Functional connectivity in the visual cortex. A paired-sample two-tailed t-test was conducted to compare zFC scores differences in CLOSED (M=0.63, SD=0.218) and OPEN (M=0.62, SD=0.181) conditions. There was no significant difference in zFC scores (t(53)=-0.42, p=0.67) between conditions. Box plot and one sample t-test map of zFC scores can be found in Figure 19 A and B.

BOLD signal change. The SPM analysis of fMRI task data revealed significant activation in the left primary visual cortex when observing flickering chequerboard presentation compared to the rest condition ($p<0.05$, FWE), see Figure 17. Other activated regions included left primary motor cortex and right primary sensory cortex, see Table 7. Contrast estimates from peak voxels of individual subjects located in the visual cortex were extracted (see Table 8) and used to later assess the relationship of task activation amplitude to neurotransmitter concentration.

BOLD signal change results			
Anatomical region	MNI coordinates (x y z)	T-value	Cluster size
Primary visual cortex (L)	-22 -98 6	15.41	9845
	-22 -90 8	15.01	
	-14 -96 -2	14.69	
Primary motor cortex (L)	-44 -10 56	10.50	725
	-58 -10 44	9.03	
Primary sensory cortex (R)	40 -26 46	9.39	1858
	58 2 40	9.33	
	60 -14 46	8.77	

Table 7: fMRI group results corrected with family-wise error at $p<0.05$ level. Only clusters larger than 100 voxels were included. Anatomical regions, MNI coordinates of local maxima, T-values and cluster sizes (in voxels) are depicted.

Participant	Contrast estimate	t-value	Participant	Contrast estimate	t-value
1	8.72	20.87	16	9.50	22.88
2	14.23	30.33	17	12.53	24.22
3	11.77	33.81	18	12.71	19.06
4	8.16	19.98	19	5.95	23.82
5	10.40	19.5	20	9.09	25.59
6	7.49	23.85	21	10.44	30.23
7	6.36	15.64	22	9.56	16.35
8	10.34	16.72	23	7.34	19.41
9	7.63	16.03	24	5.79	22.86
10	8.62	31.04	25	8.39	28.06
11	9.51	25.61	26	5.89	15.7
12	-	-	27	12.79	23.63
13	8.06	28.93	28	8.07	25.3
14	7.09	14.39	29	13.00	32.33
15	9.12	27.53	30	14.95	29.22

Table 8: Individual fMRI results. Contrast estimates and t-values corrected at $p<0.05$ are depicted.

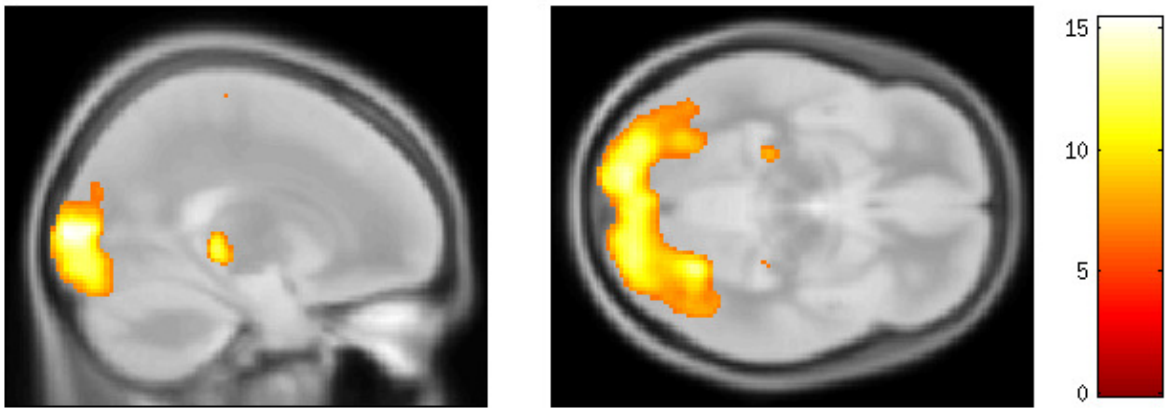

Figure 17: SPM showing task related BOLD signal increases during VIS STIM. Areas with significant fMRI activation when observing flickering chequerboard presentation compared to the rest condition are depicted ($p<0.05$, corrected). Main cluster is located in the primary visual cortex.

To summarize, no differences were found in rs-fMRI measures between the CLOSED and OPEN conditions but a significant activation of visual cortex during VIS STIM.

1.4 Relationship between local and distal neuronal activity, and neurotransmitters concentration

In the integrative MRS-fMRI analysis, we first investigated the relationship of neurotransmitter concentrations in the visual system with rs-fMRI measures of local and distal neuronal signalling during CLOSED and OPEN conditions. Next, we analysed whether GABA and Glx levels during VIS STIM were associated with the BOLD signal changes in the same brain state.

Relationship between GABA, Glx and ALFF in the visual cortex. Pearson product-moment correlation coefficients were computed to assess the relationship between

GABA, Glx and zALFF scores in CLOSED and OPEN conditions. Both neurotransmitter concentrations in the CLOSED condition did not relate to zALFF (GABA: $p>0.5$, Glx: $p>0.3$). There was a significant negative correlation between the GABA concentrations and zALFF scores in the OPEN condition ($r=-0.35$, $n=48$, $p=0.013$) but not with Glx ($p>0.7$), see Figure 18 D. In summary, GABA levels in the occipital cortex drop from intrinsic to baseline state and then correlate with the local neural activity inside the MRS voxel (measured by ALFF).

Relationship between GABA, Glx and the FC in the visual cortex. Pearson product-moment correlation coefficients were computed to assess the relationship between GABA, Glx and zFC scores in the CLOSED and OPEN conditions. Both neurotransmitter concentrations in the CLOSED condition did not relate to the FC scores (GABA: $p>0.7$, Glx: $p>0.4$). There was a significant negative correlation between GABA concentrations and zFC scores in the OPEN condition ($r=-0.32$, $n=48$, $p=0.027$) but not for Glx ($p>0.5$), see Figure 19 D. In summary, GABA levels in the occipital cortex correlate with the intrinsic visual cortex connectivity in the baseline, but not in the intrinsic brain state.

Overall, we found that the levels of GABA drop from the intrinsic to baseline states and that baseline GABA concentration correlates with local and distant measures of neuronal activity across subjects. Glx did not change between the intrinsic and baseline states and has no relationship with the neuronal activity as measured with fMRI.

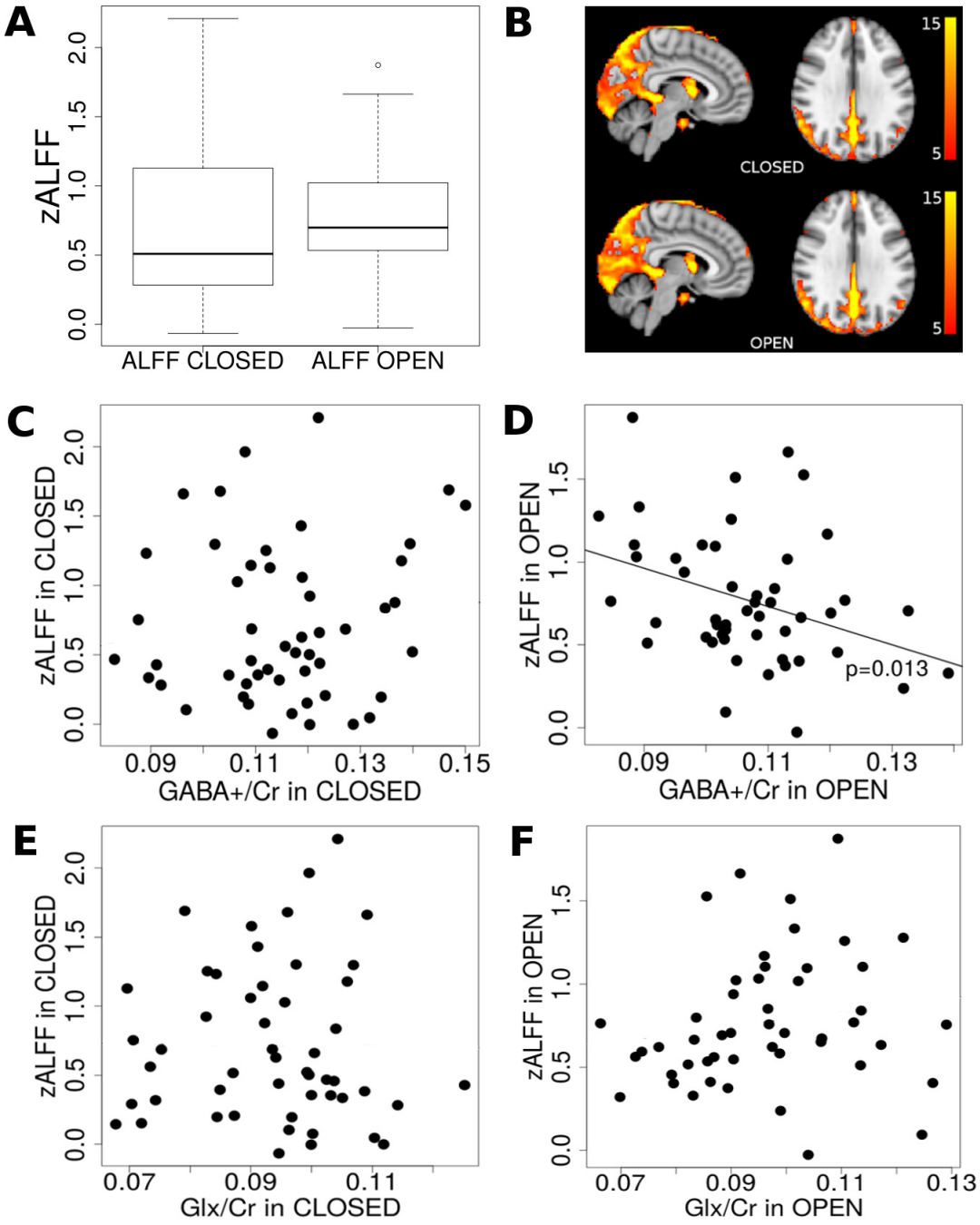

Figure 18: Local neuronal activity and concentrations of neurotransmitters. (A) Box plot of group zALFF CLOSED and zALFF OPEN scores. (B) One sample t-test map of zALFF scores in the CLOSED and OPEN conditions (p=0.05). zALFF scores were derived from the ROIs corresponding to the placement of MRS voxels for individual subjects. (C) Relationship between the zALFF scores and GABA+/Cr in the CLOSED condition. (D) Significant correlation (p=0.013) between the zALFF scores and GABA+/Cr in the OPEN condition. (E) Relationship between the zALFF scores and Glx/Cr in the CLOSED condition. (F) Relationship between the zALFF scores and Glx/Cr in the OPEN condition.

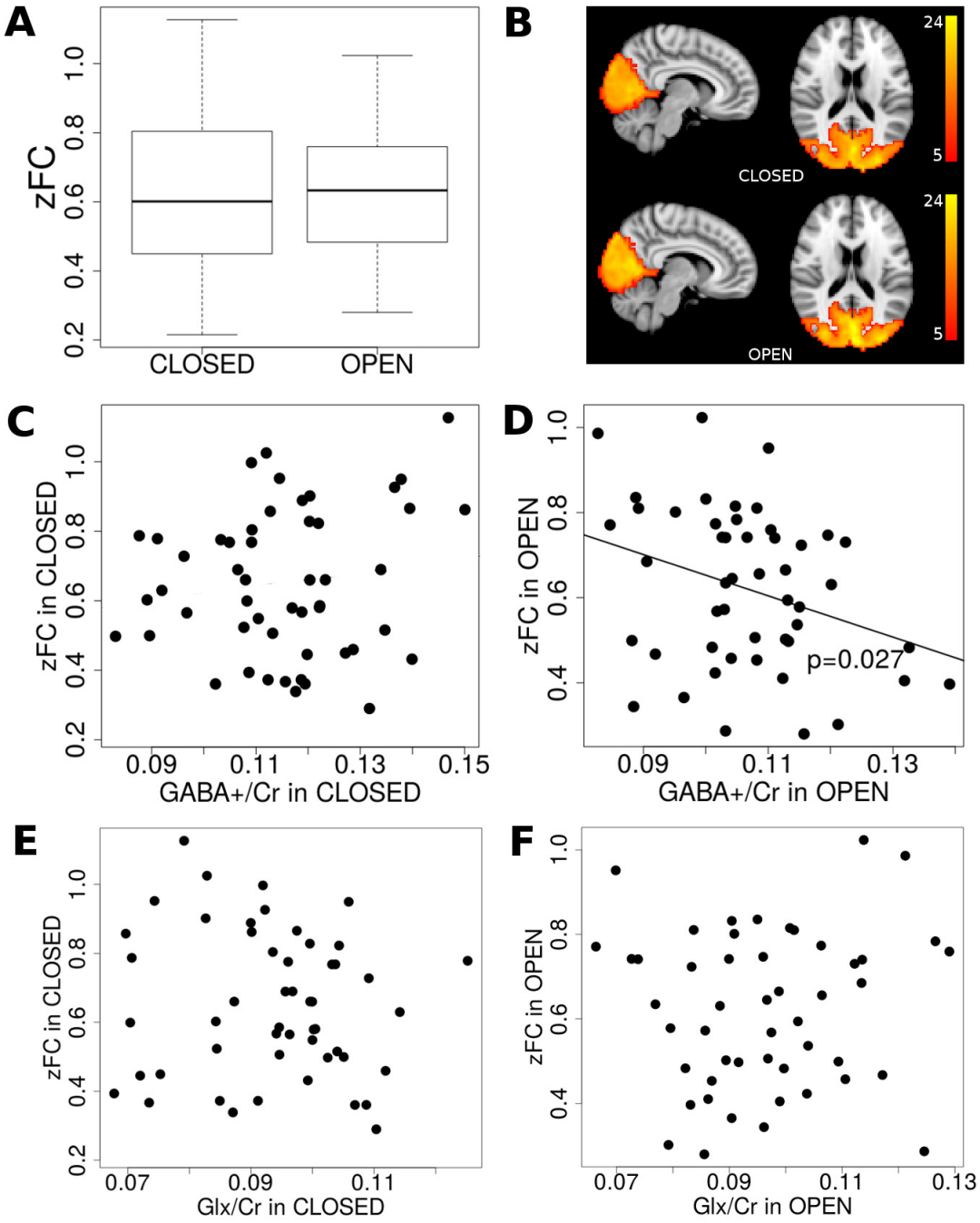

Figure 19: Functional connectivity and concentrations of neurotransmitters. (A) Box plot of group zFC CLOSED and zFC OPEN scores. (B) One sample t-test map of zFC scores in the CLOSED and OPEN conditions (p=0.05). (C) Relationship between the zFC scores and GABA+/Cr in the CLOSED condition. (D) Significant correlation (p=0.027) between the zFC scores and GABA+/Cr in the OPEN condition. (E) Relationship between the zFC scores and Glx/Cr in the CLOSED condition. (F) Relationship between the zFC scores and Glx/Cr in the OPEN condition.

Relationship between GABA, Glx and BOLD signal change in the VIS STIM condition. Pearson product-moment correlation coefficients were computed to assess the relationship between GABA, Glx and contrast estimates of the BOLD signal changes in the VIS STIM condition. The GABA concentrations in the VIS STIM condition did not relate to BOLD signal changes (r=-0.28, n=28, p=0.14). However, there was a significant positive correlation between Glx concentrations and BOLD contrast estimates in the VIS STIM condition (r=0.41, n=28, p=0.03), see Figure 20. In summary, the glutamate concentration in the VIS STIM state relates to the fMRI activity arising from observing the chequerboard stimulation.

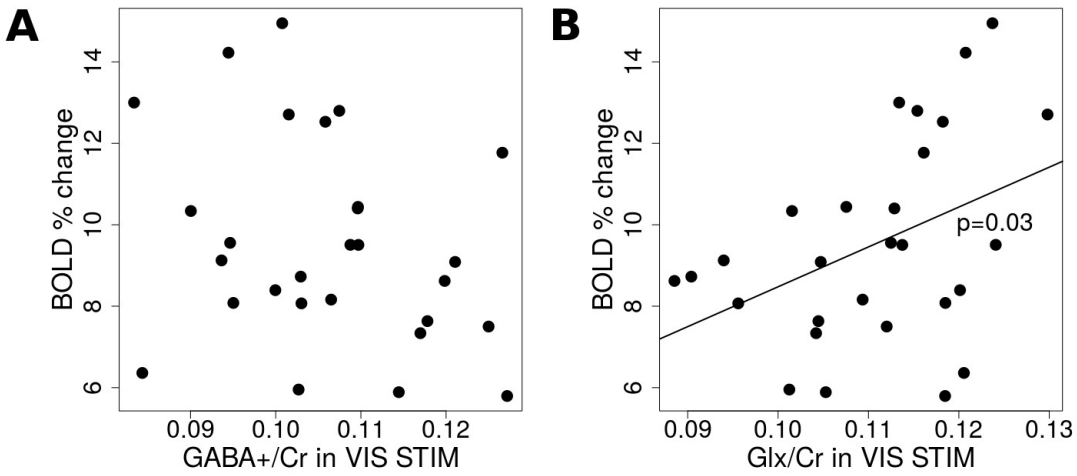

Figure 20: Relationship between the BOLD percent signal change, GABA+/Cr (A), and Glx/Cr (B) concentration in the occipital cortex in VIS STIM condition.

1.5 Results of behavioural experiments

Orientation discrimination task. The individual performance in orientation discrimination was determined for all participants and averaged to 7.1° (SD=4.18°, min=2.14, max=17.03). Five volunteers were not able to discriminate any of the tilt angles above the chance level, most probably because they could not see a very briefly (25 ms) presented

Gabor patch without an extensive training.

Attentional capture task. Overall task response accuracy of all subjects was calculated and amounted to 94.0% in average. Error rates were equal for both: distractor absent and present conditions comprised of 15 erroneous trials in all blocks. Mean reaction times (RTs) were calculated after excluding error trials. The mean RT of a distractor absent trial was 986 ms, and the mean RT of a distractor present trial was 1127 ms. A paired-sample one-tailed t-test was conducted to compare differences in response reaction times between the distractor-present and distractor-absent trials which revealed a significant difference between the two conditions ($t(27)=8.38$, $p=0.001$).

1.6 Relationship between behaviour and neurotransmitters concentration

Here, we analysed whether the neurotransmitter concentrations in the VIS STIM condition related to the basic visual performance (orientation discrimination task) and not to the attention-related processing task (attentional capture search).

Relationship between GABA, Glx and orientation discrimination task performance. Pearson product-moment correlation coefficients were computed to assess the relationship between GABA and Glx in VIS STIM condition, and the performance of the orientation discrimination task. There was a significant negative correlation between GABA concentration in VIS STIM condition and GABOR patch tilt angles discrimination ($r = -0.54$, n=23, p=0.008), see Fig. 21 A. There was no significant correlation between Glx concentration and orientation discrimination task performance. In summary, the GABA but not the Glx concentration during visual processing predicted orientation

discrimination performance.

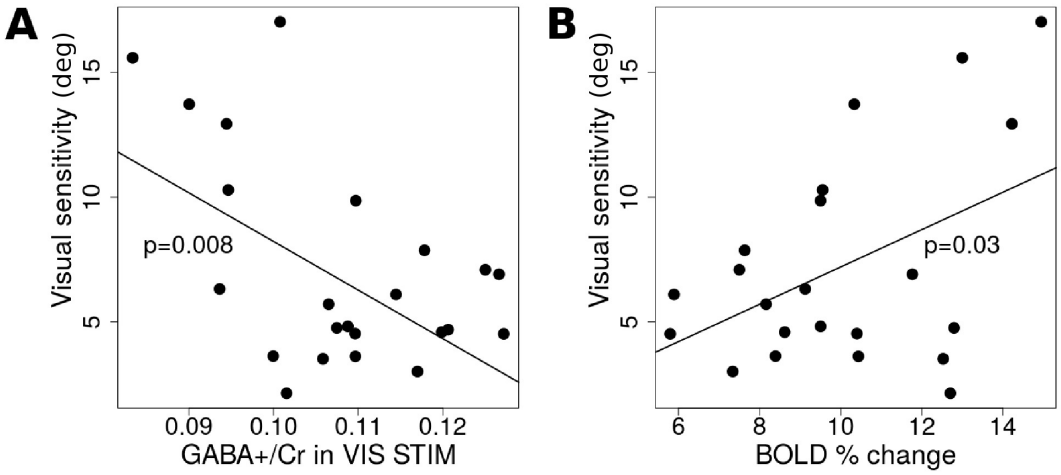

Figure 21: (A) Significant correlation (p=0.008) between GABA+/Cr concentrations in VIS STIM condition and visual sensitivity, measured by performance in orientation discrimination. (B) Significant correlation (p=0.03) between BOLD signal changes and visual sensitivity in individual subjects. Note that discrimination of smaller angles (deg) reflects a better visual sensitivity.

Relationship between GABA, Glx and attentional capture task performance. Pearson product-moment correlation coefficients were computed to assess the relationship between GABA, Glx and RTs of the attentional capture task. There were no significant correlations found. In summary, neither GABA nor Glx concentration predicted attentional capture search performance.

1.7 Relationship between behaviour and fMRI measures

In the final step, we analysed the relationships between the behavioural experiments and the fMRI measures. The orientation discrimination task employs basic visual signalling

processes, so we assessed the correlation between its performance and the BOLD signal change in VIS STIM condition.

Relationship between orientation discrimination task performance and BOLD signal change. Pearson product-moment correlation coefficient was computed to assess the relationship between the performance in orientation discrimination and the BOLD signal change in the VIS STIM condition. There was a significant positive correlation between the GABOR patch tilt angles discrimination and the contrast estimate values of the BOLD signal ($r=0.42$, $n=22$, $p=0.03$), see Figure 21 B. In summary, fMRI activity in the VIS STIM condition correlated negatively with the visual discrimination performance.

Relationship between attentional capture task performance and BOLD signal change. Pearson product-moment correlation coefficients was computed to assess the relationship between the performance in attentional capture search and the BOLD signal change in the VIS STIM condition. There were no significant correlations found between variables.

Overall, the performance in the orientation discrimination task but not in the attentional capture search reflected BOLD signal change in the VIS STIM condition.

2 Experiment 2. Modulation of neurotransmitters by transcranial magnetic stimulation

In order to assure that the effects of TMS are comparable across conditions, we assessed the time interval between the end of TMS session and the start of the MR acquisition. Average interval was 6 minutes and 54 seconds (SD=1.1 min, MIN=5 min 20 sec, MAX=13 min). As assessed with paired-sample two-tailed t-tests, no significant differences in time between the pre-TMS, post-TMS_{lAG}, and post-TMS_{IPL} conditions were found.

2.1 Modulation of GABA and Glx by the TMS intervention

In the following paragraphs we report differences in the neurotransmitter concentrations between the pre-TMS, post-TMS_{lAG}, and post-TMS_{IPL} conditions. As discussed in section 3.1.2 of the materials and methods part, referencing GABA peak to water (GABA/H_2O) yields better results accuracy than analysing GABA/Cr concentrations. We therefore present both GABA concentration changes across states.

GABA/H_2O concentration. A one-way between subjects ANOVA revealed a significant effect of TMS on GABA/H_2O concentrations between conditions ($F(2, 81)=7.01$, $p=0.001$). Post-hoc paired-sample two-tailed t-tests revealed a significant decrease in GABA concentration between the pre-TMS (M=2.31, SD=0.194) and post-TMS_{lAG} (M= 2.14, SD=0.284) conditions ($t(25)=-3.8$, $p=0.0016$, corrected for multiple comparisons) but not between pre-TMS and post-TMS_{IPL} conditions ($p>0.4$), see Figure 22. In average, signal dropped by 20.19%. The group averaged GABA/H_2O concentrations can be found in Table 9 A.

(A) Group averaged concentrations of GABA anf Glx with standard deviations			
Group	GABA/H_2O (SD)	GABA+/Cr (SD)	Glx/Cr (SD)
pre-TMS	2.31 (0.194)	0.100 (0.0083)	0.091 (0.0016)
post-TMS_{lAG}	2.14 (0.284)	0.094 (0.0132)	0.092 (0.0089)
post-TMS_{IPL}	2.38 (0.251)	0.104 (0.0126)	0.088 (0.0113)
(B) Group averaged FWHM values and standard deviations			
Group	pre-TMS (SD)	post-TMS_{lAG} (SD)	post-TMS_{IPL} (SD)
GABA FWHM	19.47 (1.293)	19.61 (1.558)	20.12 (2.236)
Glx FWHM	14.79 (1.425)	15.04 (1.665)	14.13 (0.991)
(C) Shapiro test results: W-scores and p-values			
Group	GABA/H_2O (SD)	GABA+/Cr (SD)	Glx/Cr (SD)
pre-TMS	W=0.976, p=0.46	W=0.950, p=0.17	W=0.977, p=0.75
post-TMS_{lAG}	W=0.953, p=0.27	W=0.959, p=0.30	W=0.961, p=0.32
post-TMS_{IPL}	W=0.977, p=0.77	W=0.957, p=0.28	W=0.979, p=0.80
(D) Pearson correlation coefficients and p-values			
Group	pre-TMS	post-TMS_{lAG}	post-TMS_{IPL}
GABA/Cr×Glx/Cr	-0.02 (p=0.92)	-0.33 (p=0.074)	-0.05 (p=0.79)

Table 9: Group averaged spectroscopy results in the pre-TMS, post-TMS_{lAG} and post-TMS_{IPL} conditions. (A) Group averaged GABA/H_2O, GABA+/Cr and Glx/Cr concentrations. (B) Group averaged FWHM scores of GABA and Glx peaks. (C) Shapiro tests results. (D) Pearson correlation coefficients between GABA+/Cr and Glx/Cr.

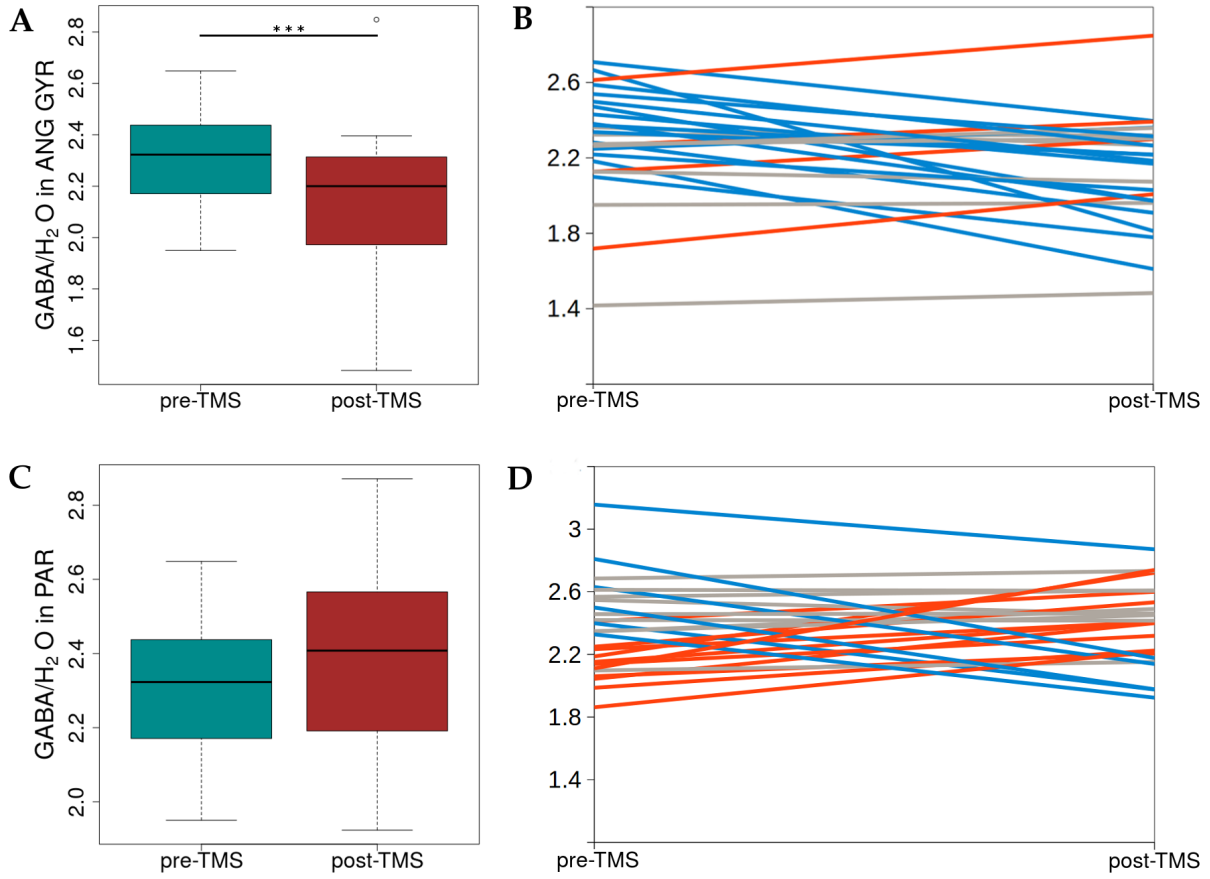

*Figure 22: (A,C) Box plots of group $GABA/H_2O$ concentration distributions before and after the TMS intervention in the angular gyrus (A) and in the parietal cortex (C); statistically significant difference is marked with *** ($p<0.001$); (B,D) Changes in $GABA/H_2O$ in individual subjects; red line depicts $\geqslant$ 5% concentration increase between conditions, blue line: $\geqslant$ 5% decrease; if the metabolite concentration change was $\leqslant$ 5%, a gray line was drawn.*

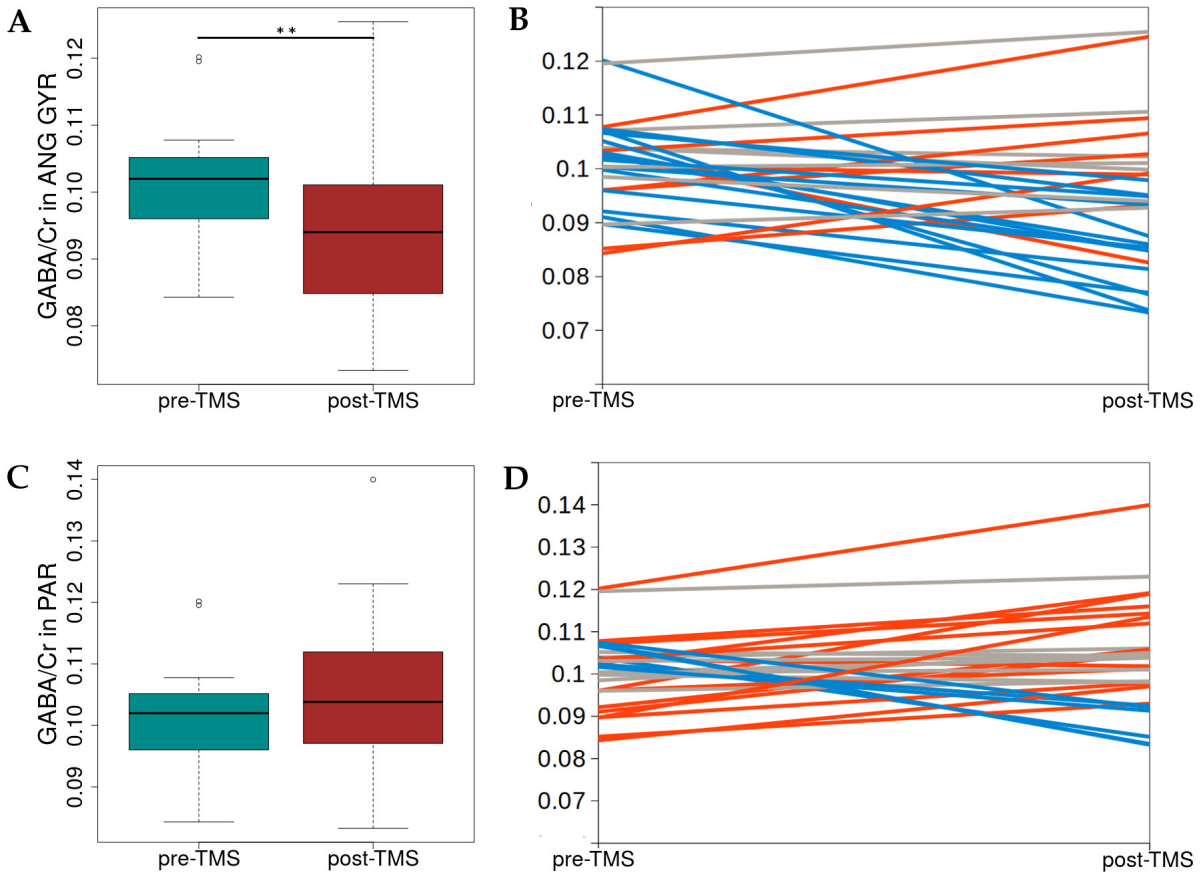

*Figure 23: (A,C) Box plots of group GABA/Cr concentration distributions before and after the TMS intervention in the angular gyrus (A) and in the parietal cortex (C); statistically significant difference is marked with ** ($p = 0.01$); (B,D) Changes in GABA/Cr in individual subjects; red line depicts $\geqslant$ 5% concentration increase between conditions, blue line: $\geqslant$ 5% decrease; if the metabolite concentration change was $\leqslant$ 5%, a gray line was drawn.*

GABA/Cr concentration. A one-way between subjects ANOVA revealed a significant effect of TMS on GABA/Cr concentrations between conditions (F(2, 85)=4.45, p=0.014). Post-hoc paired-sample two-tailed t-tests revealed a significant GABA concentration decrease between pre-TMS (M=0.100, SD=0.0083) and post-TMS_{lAG} (M=0.094, SD=0.0132) conditions (t(28)=-2.87, p=0.016, corrected for multiple comparisons) but not between pre-TMS and post-TMS_{IPL} conditions (p>0.5), see Figure 23. In average, signal dropped by 9.19%. The group averaged GABA/Cr concentrations can be found in Table 9 A.

Glx/Cr concentration. A one-way between subjects ANOVA revealed no effects of TMS on Glx concentrations between pre-TMS, post-TMS_{lAG}, and post-TMS_{IPL} conditions (F(2, 87)=2.34, p=0.10). Box plots representing group results are depicted in Figure 24. The group averaged Glx concentrations can be found in Table 9 A.

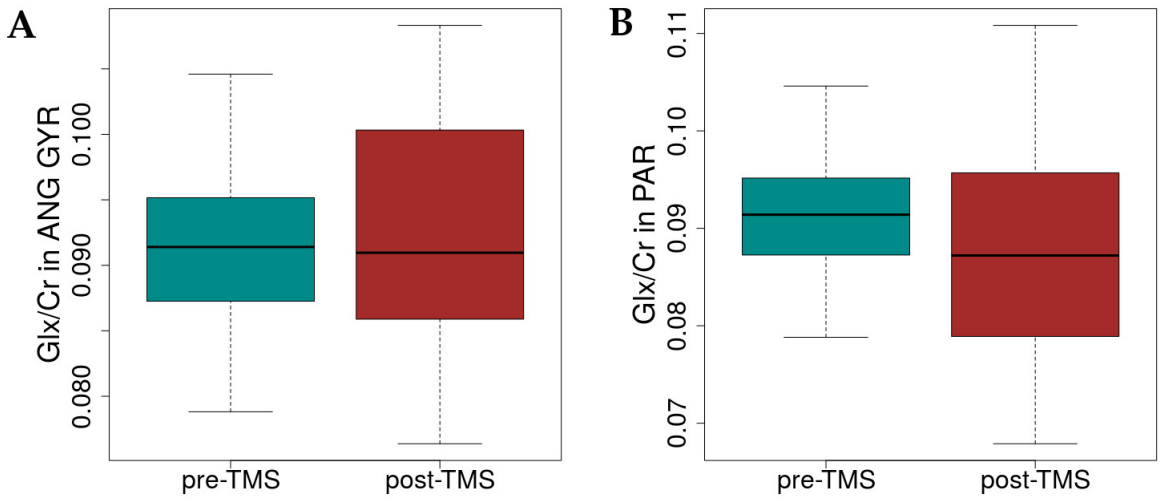

Figure 24: Box plots of group Glx/Cr concentrations distribution before and after TMS intervention in the angular gyrus (A) and in the parietal cortex (B).

In summary, the TMS_{lAG} intervention decreased the GABA concentration in the visual system. In contrast, the TMS_{IPL} did not affect the neurotransmitter concentrations. Next, we performed control analyses to verify the effects of the GABA and Glx linewidth stability, the normality of the distribution and the correlation between the neurotransmitters on the differences in neurotransmitter concentrations across the conditions.

GABA and Glx peak width. A one-way between subjects ANOVA was conducted to compare the effects of TMS stimulation on linewidths of GABA and Glx peaks (FWHM) in pre-TMS, post-TMS_{lAG}, and post-TMS_{IPL} conditions. There was no significant effect of the intervention on GABA FWHM ($F(2, 87)=0.68$, $p=0.51$). There was a significant effect of condition on Glx FWHM ($F(2, 87)=3.45$, $p=0.036$). However, post-hoc paired-sample two-tailed t-tests revealed no significant difference in Glx FWHM between the pre-TMS ($M=14.79$, $SD=1.425$) and post-TMS_{lAG} ($M=15.04$, $SD=1.665$) conditions ($t(29)=0.86$, $p=0.39$) and a marginally significant drop in Glx FWHM between pre-TMS and post-TMS_{IPL} ($M=14.13$, $SD=0.991$) conditions ($t(29)=-1.97$, $p=0.058$) that did not survive the correction for multiple comparisons. The group averaged FWHM values can be found in Table 9 B.

Normality of the group results distribution. GABA and Glx group results in three conditions were tested for violation of normality of the distribution with the Shapiro-Wilk test ($p<0.05$). All group values were distributed normally. The group W-scores and p-values can be found in Table 9 C.

Correlation between the GABA and the Glx concentrations. Pearson product-moment correlation coefficients were computed to assess the relationship between GABA and Glx values in each of the three conditions. There was a marginally significant nega-

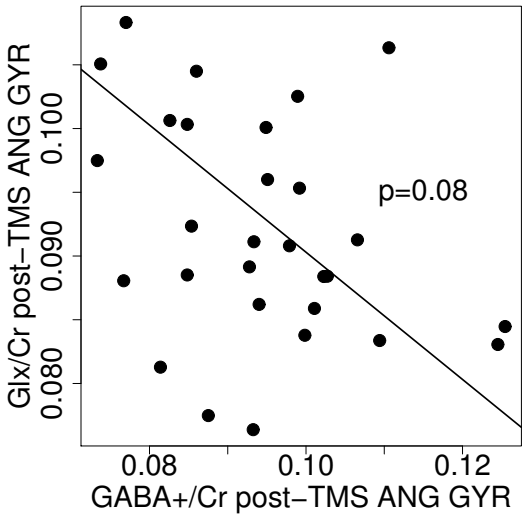

Figure 25: Relationship between GABA/Cr and Glx/Cr concentration after the TMS intervention in the angular gyrus.

tive correlation between GABA and Glx in the post-TMS_{lAG} condition (r=-0.33, n=30, p=0.074), see Figure 25. There were no significant correlations between those variables in the pre-TMS and the post-TMS_{IPL} conditions. Pearson product-moment correlation coefficients and p-values can be found in Table 9.

To summarize, the control analyses revealed no significant changes in GABA and Glx linewidth stability and the normality of the distribution between conditions. There was a marginally significant correlation found between the neurotransmitter concentrations in the post-TMS_{lAG} condition.

2.2 Modulation of other metabolites by the TMS intervention

One-way between subjects ANOVAs were conducted to compare the effect of TMS stimulation on Asp, GSH, Ins, PCh and NAA concentrations in the three conditions. There was no significant effect of the TMS intervention on those metabolites at the $p<0.05$ level,

Group averages of metabolites concentrations in the "edit-off" spectrum.				
Metabolite	pre-TMS	post-TMS_{lAG}	post-TMS_{IPL}	ANOVA
Asp	0.24 (0.036)	0.25 (0.046)	0.24 (0.058)	F=0.33, p=0.72
GSH	0.21 (0.020)	0.21 (0.025)	0.22 (0.042)	F=1.28, p=0.28
Ins	0.78 (0.055)	0.78 (0.057)	0.81 (0.087)	F=1.89, p=0.16
GPC+PCh	0.15 (0.013)	0.15 (0.014)	0.14 (0.011)	F=0.91, p=0.41
NAA+NAAG	1.51 (0.082)	1.51 (0.092)	1.52 (0.104)	F=0.29, p=0.75

Table 10: Group averaged metabolites concentrations in the "edit-off" spectrum in the pre-TMS, post-TMS_{lAG} and post-TMS_{IPL} conditions. Standard deviation values are given in brackets. One-way between subjects ANOVAs scores comparing metabolite concentrations in three conditions are shown in the last column.

which suggests that the changes in brain states only affected the GABA neurotransmitter and not other metabolites. The group averaged metabolite concentrations can be found in Table 10.

2.3 fMRI measures before and after the rTMS

The effects of the TMS intervention on the connectivity within brain networks were assessed. The IPL connects with the occipital cortex via top-down connections [101], so we examined the effects of TMS_{IPL} on the visual network's iFC. The lAG is a part of the default mode network (DMN) and is functionally related to the dorsal attention network (DAN) [47, 118], so we investigated the effects of TMS_{lAG} on the DAN's iFC.

Visual and dorsal attention network connectivity before and after the TMS intervention. Paired-sample two-tailed t-tests were conducted to compare ICA scores differences between the pre-TMS and post-TMS conditions. After the rTMS intervention in the parietal cortex, there was a marginally significant decrease in iFC of the visual network between pre-TMS (M=4.39, SD=0.482) and TMS_{IPL} (M=4.22, SD=0.468) conditions (t(24)=-1.85, p=0.076), see Figure 26 B. After the rTMS intervention to the angular gyrus, there was a significant increase in iFC of the DAN between pre-TMS (M=3.78, SD=0.226) and TMS_{lAG} (M=3.93, SD=0.229) conditions (t(24)=3.32, p=0.002), see Figure 26 C. To summarize, TMS_{IPL} intervention decreased iFC of the visual network, whereas TMS_{lAG} elevated iFC of the DAN.

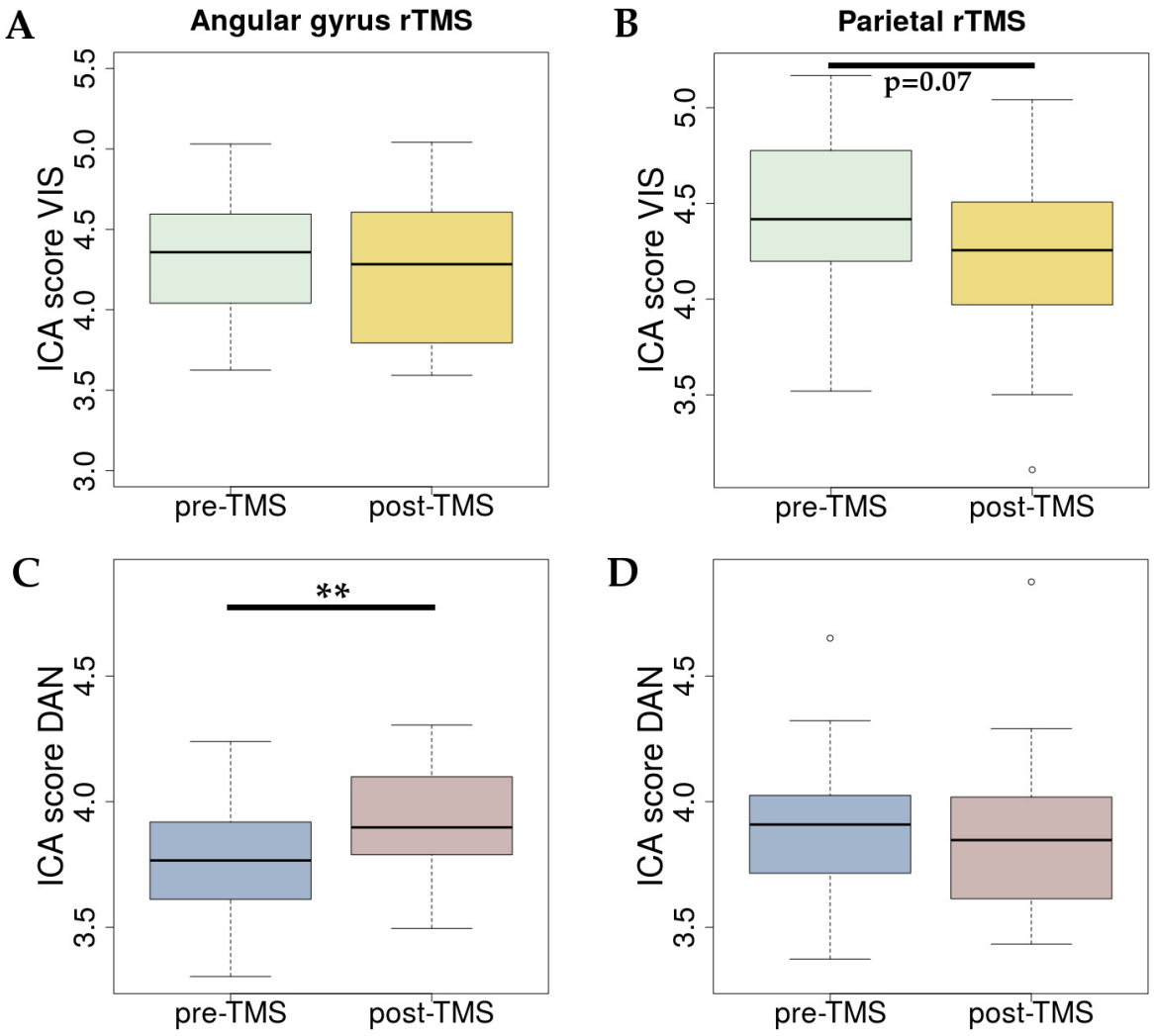

Figure 26: Modulation of network connectivity after the TMS stimulation. (A) ICA scores in the visual network before and after the TMS_{lAG}. (B) Marginally significant (p=0.07) decrease of the visual network connectivity after the intervention in the TMS_{IPL}. (C) Significant increase of the dorsal attention network (DAN) connectivity after TMS_{lAG}. (D) ICA scores in the DAN before and after the TMS_{IPL}.

Part V

Discussion

1 Experiment 1. The role of GABA and Glu in the visual system

The goal of this study was to systematically investigate GABA and Glx neurotransmitter concentrations in the visual cortex in different brain states, and to relate them to the fMRI measures and visual performance. Three brain states were studied with increasing visual input: eyes closed (CLOSED), eyes open (OPEN) in darkness and eyes open with visual stimulation (VIS STIM).

1.1 Changes in GABA and Glx across brain states

We found different dynamics of both GABA and Glx across behavioural states. GABA concentration decreased from the CLOSED to OPEN states and Glx concentration increased from the CLOSED to VIS STIM states. In the following, I will discuss these changes in relation to different states of neuronal signalling and possible confounding effects.

1.1.1 GABA decreases from CLOSED to OPEN states with no further change during VIS STIM

GABA concentration decreased from the CLOSED to OPEN state with no further change in the VIS STIM condition. This is the first report showing that the inhibitory neurotrans-

mitter concentration in the visual system drops after simply opening the eyes in darkness. A neurophysiological analogue of this effect is a drop in alpha frequency power of the EEG signal observed after opening the eyes [5]. Particularly, as EEG alpha rhythm is generated by neuronal GABAergic activity stimulating low-threshold T-type voltage-gated calcium channels [60, 72]. A possible role of elevated GABAergic neurotransmission in the CLOSED state is the synchronized inhibition of distant networks in the absence of visual stimulation. After opening the eyes, even with low sensory input during darkness, the visual system is prepared to process sensory signals locally and through communication with other brain regions, thus decreased GABAergic inhibition enables these processes. A similar shift between internal and external processing was observed in synchronized oscillatory activity of EEG and MEG data [48, 64, 89, 119].

On the molecular level, this observed change in GABA-ergic transmission might reflect one of the following two cellular processes: decrease of GABA production (mediated by glutamate decarboxylase - GAD) or increase of GABA reuptake and catabolism. If GABA re-uptake and catabolism was the underlying process, the GABA drop would be accompanied by an immediate increase of the Glx signal (due to increased GABA conversion to Glu in astrocytes, see the depiction of GABA/Glu cycle on Figure 27). Since we did not observe this effect in our simultaneous GABA- and Glx-measurement, the decrease of GABA production appears to be the more likely mechanism of the GABA dynamics [38, 68].

After GABA decreased with opening the eyes, we found no further change between the OPEN and VIS STIM states. Nonetheless, Mekle et al. recently reported a significant GABA reduction in the occipital cortex after applying visual stimulation to the contralateral hemisphere [80]. In their experiment, the MRS signal was acquired on a more

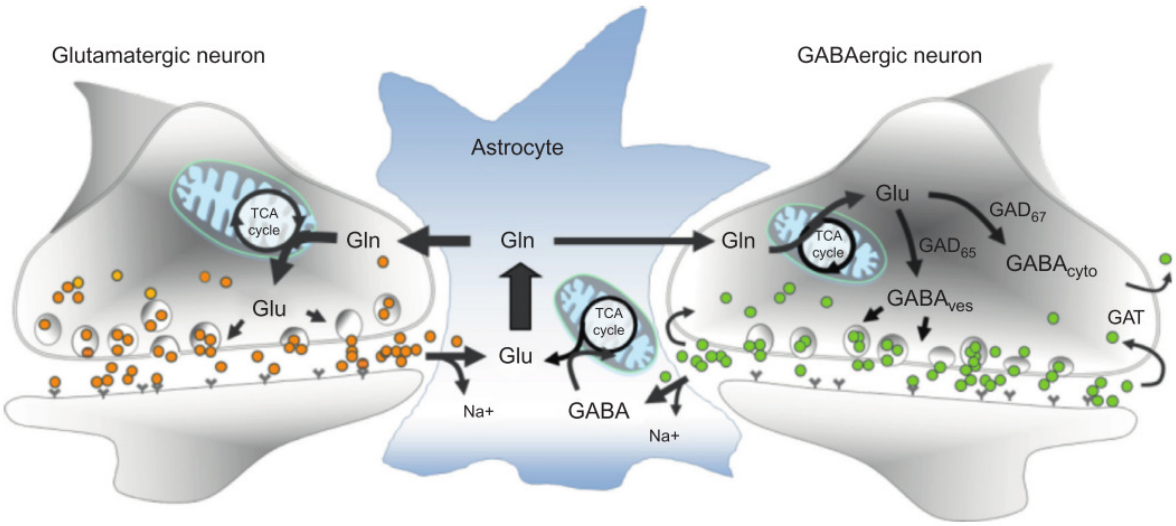

Figure 27: Depiction of GABA/glutamate and glutamine circle between GABAergic neuron, glutamatergic neuron and astrocyte. GABA and glutamate (Glu) are released from neurons during neural activity. Glutamate is transported to astrocytes via membrane transporters, while GABA can additionally be reaptaken directly to GABAergic terminals. In astrocyte, glutamate cycle includes conversion into glutamine (Gln), which is later packaged into vesicles and transported back to glutamaergic neurons. GABA metabolism includes tricarboxylic acid (TCA) cycle and conversion into glutamate and later processing to glutamine. Following the Gln transport to GABAergic neuron, glutamine is converted in the TCA cycle to Glu. To finalize the cycle, GABA is synthesized from Glu by glutamate decarboxylase (GAD) and loaded into synaptic vesicles. Adapted from Sibson and Behar, 2014 [105].

sensitive 7T system with higher signal to noise ratio (SNR) as compared to a 3T scanner. Nevertheless, other studies on 7T systems also found no GABA changes in the occipital cortex between baseline and visual stimulation conditions [12, 75, 104]. An imprecise definition of the baseline condition itself could explain the diverging results. We therefore systematically studied GABA in different brain states. Our finding of different GABA dynamics during several states without visual input suggests that GABA levels rather reflect a system's preparation for upcoming than real visual input. Proper definitions of baseline states (eyes closed or open) are therefore essential to study GABA-ergic changes and might explain inconsistent reports so far.

1.1.2 Glx increases from CLOSED to VIS STIM states

Glx concentration increased from the CLOSED to VIS STIM states but did not change between CLOSED and OPEN states. The upregulation of excitatory neurotransmission in the occipital cortex during visual stimulation has already been shown in recent studies on 7T systems [12, 56, 75, 104]. Such Glx increase was accompanied by Lac and Asp [12, 75, 80, 103] both associated with the TCA cycle [75]. This suggests that increased glutamatergic neurotransmission might be related to the elevated oxidative metabolism and energetic demands in the occipital cortex while processing visual input. This is supported by PET studies reporting increased oxidative metabolism and glucose consumption in the occipital cortex when processing visual input [7, 67, 82]. Our results therefore support the thesis that the task-related Glx increase in the visual cortex is of signalling origin [54, 55]. Task related increases of Glx have not only been observed in sensory but also higher-order brain regions. Cognitive task performance was reported to up-regulate the Glx levels in the cingulate cortex during a Stroop task [115] and in the medial prefrontal cortex (mPFC) during a mental imagery task [54].

1.1.3 Control analyses

In the following, I will discuss unspecific variations in MRS parameters that might explain the dynamics we observed in the GABA and Glx concentrations. In order to evaluate those effects, we performed several control analyses.

Changes in metabolites across behavioural states might be simply related to blood flow changes which would substantially impact on the peak width (FWHM) of both GABA and Glx peaks. Furthermore, FWHM changes might occur due to changes in local magnetic susceptibility. However, we found no variance of the FWHM of GABA and Glx between the CLOSED, OPEN and VIS STIM conditions which speaks against previous interpretations. Stable FWHM across brain states also rules out artefacts caused by head movements (which reduce the coupling between the head and the radiofrequency coil) and speaks in favor of signalling related changes in neurotransmitter concentrations across brain states [38].

It is still discussed in the literature whether the two neurotransmitter signals are resolved independently from each other or whether they are highly coupled within an MRS acquisition [83]. We therefore, for the first time, analysed both signals during identical states and separately and independently quantified GABA and Glx peak integrals from the edited spectrum. We then assessed the relationship between both neurotransmitters but found no significant correlations across conditions. This suggests that GABA and Glx peaks from the edited spectrum depict distinct molecules.

Lastly, we investigated whether the dynamics of GABA and Glx concentrations were specific for these neurotransmitters. In control analyses we found no further changes across conditions for other metabolites including Asp, GSH, Ins, PCh and NAA, and therefore suggest a specific decrease of GABA from CLOSED to OPEN and a specific

increase of Glx from CLOSED to VIS STIM conditions.

1.2 Relationship between neuronal activity and neurotransmitter concentrations

We found significant relationships between neurotransmitter concentrations and neural activity measured with BOLD. In the OPEN condition, the GABA concentration correlated negatively with local neuronal activity (measured with ALFF and FC). In the VIS STIM condition, Glx correlated positively with BOLD signal changes. This is the first study to directly relate both MRS-derived neurotransmitter levels with BOLD signal changes in the visual cortex across brain states.

1.2.1 Baseline GABA concentrations and ongoing neuronal activity

The GABA concentration in the occipital cortex dropped from CLOSED to OPEN condition and then correlated negatively with the ALFF and FC scores in the same region. To my knowledge, this is the first study reporting a relationship between local fMRI measures and neurotransmitter concentrations in the visual system. Few studies have so far investigated the associations between GABA levels and rs-fMRI signals in other regions than the visual cortex of the healthy brain. In those reports, the local GABA concentration correlated negatively with iFC in the motor cortex [4, 111], in the anterior cingular cortex (ACC) [88] and in the DMN [61]. These findings support the role of GABAergic inhibitory neurotransmission in regulating spontaneous neural activity as measured with rs-fMRI.

Although the relationship between GABA and fMRI measures has only recently been studied, others report correlations between GABA and oscillatory activity measured with

magnetoencephalography (MEG). MEG records magnetic fields produced by electrical currents occurring naturally in the brain during rest and while performing a task [45]. Studies found a positive correlation between gamma oscillatory frequency during processing of visual grating stimuli and GABA concentration in the occipital cortex [36, 85] while others could not replicate this finding [25]. Other groups suggest that ongoing oscillatory activity in beta and gamma bands is possibly mediated by GABAergic neurotransmission [17, 44]. Moreover, in a PET study, Kujala et al. showed that $GABA_A$ receptor density in the primary visual cortex correlates negatively with the amplitude of visually induced gamma oscillations measured with MEG [66].

To conclude, previous reports indicate an important role of inhibitory neurotransmission in maintaining intrinsic baseline activity in the visual cortex. Our study adds to this notion by finding a decrease of GABAergic signalling from an undisturbed intrinsic state with eyes closed to a preparatory state expecting visual input during eyes open in darkness.

1.2.2 Task related increase of Glx concentrations and local neuronal activity

We found a significant positive correlation between the Glx concentration in the occipital cortex and the BOLD signal change in the same region in the VIS STIM condition. This is in line with previous reports from 7T scanners that also found positive relationships between the Glx concentration and task related BOLD-fMRI signal change in the occipital cortex [11, 56]. Our results indicate that a larger sample size reveals identical correlations even on a 3T system.

No further studies exist on a possible relationship between changes of Glx and fMRI signals from the healthy brain. However, several studies identified correlations between iFC measures and Glx concentrations in the diseased brain. E.g. increased correlations

were observed between Glx and the ALFF score in the prefrontal cortex of patients suffering from major depression [130]. Others found elevated correlations between Glx and prefrontal iFC in endometriosis-associated chronic pelvic pain (CPP) patients [3]. The enhanced glutamatergic neurotransmission related to increased iFC might play a key role in a disruption of systems-level brain dynamics.

Although Glx related to BOLD signal change during VIS STIM, we found no significant correlation between GABA and BOLD in the same condition, which is in line with the recent finding by Harris [49]. However, few previous studies reported such a relationship during similar yet different settings [11, 32, 85]. One difference is that earlier reports were based on samples of only 10-15 participants while we extended our sample to 30 healthy volunteers. Another discrepancy are different methodologies to extract BOLD signal changes from the fMRI data. Finally, the most critical difference is that earlier studies did not precisely define their baseline condition. As we showed in this study, GABA changes from CLOSED to OPEN and diverging control conditions in earlier studies might be the reason for the differences found.

1.3 Relationship between behaviour and neurotransmitters concentrations

In the present study the GABA levels in the occipital cortex positively correlated with the orientation discrimination but not with the attentional capture performance. It suggests that the inhibitory capacity of the visual system predicts the performance in a low-level (orientation discrimination), but not in a high-level (attentional capture) visual processing task. This results confirms previous reports which positively correlated the performance in the orientation discrimination with the GABA concentration [36, 85, 128].

The role of GABA in the discrimination performance might be to regulate the oscillatory processes in the visual system. The temporal coding of visual input, determined by bottom-up and top-down processes, is coordinated by alpha and gamma oscillations, which (as mentioned in section 1.1.1 of this discussion) are generated by the GABAergic inhibitory activity [58].

The relationship between visual performance and the GABAergic neurotransmission was as well reported in animal studies where $GABA_A$ receptors concentration related to sensitivity and selectivity of V1 neurons [62]. Together with our results (and results from other studies) it suggests that the GABA inhibition plays a fundamental role in establishing selectivity for stimulus orientation.

GABA also regulates function of other brain regions apart from visual cortex. In the study by Greenhouse et al. the excitability of the motor system (measured with MEG) correlated negatively with the GABA concentration, and positively with speed in the motor task [42]. The authors suggest that the GABA suppresses an over-reactive motor system and thereby increases its performance. Possibly, the analogous enhanced GABAergic inhibition of the visual system allows for better precision in the orientation discrimination task through GABA-induced selectivity of visual input.

1.4 Study limitations

One of the study limitations is the sequential (and not concurrent) acquisition of MRS and fMRI signals. Implementation of simultaneous MRS-fMRI pulse sequence would allow a more accurate comparison between the neurotransmitter levels and neural activity. Thanks to recent developments in pulse sequences, concurrent Glx-fMRI data can be collected on the 3T system [1]. However, the simultaneous acquisition of both neuro-

transmitters (GABA and Glx) in addition to the fMRI signal at this field strength is currently not feasible. With further technical advancements it should be soon possible on the 7T scanners using short-TE sequences [35].

Another limitation of the study was that the acquisition of the neuroimaging and behavioural data took place in separate sessions. Behavioural experiments employed complex set-up, including the eye-tracking system and a precise interval of stimulus presentation on the display. These settings could not be implemented in the scanner so the testing was performed in the psychological laboratory on a different date.

2 Experiment 2. Modulation of neurotransmitter concentrations by TMS

The goal of this study was to systematically investigate the effects of non-invasive, inhibitory TMS intervention on the neurotransmitter concentrations in the occipital cortex, and on fMRI fluctuations inside and outside the visual system. Two regions were stimulated: IPL in the parietal cortex (as part of dorsal visual stream) and the lAG - a part of the DMN outside the visual stream. Based on the network directionality model, parietal and occipital regions exert a top-down effect on visual cortex. We therefore analysed whether the TMS inhibition of top-down region would decrease the connectivity in the visual system and affect neurotransmitter concentrations.

We started by assessing the average time interval between the pre-TMS and post-TMS sessions in different conditions. In a pilot experiment, Castrillon and Riedl (unpublished) found that the effect of inhibitory rTMS on the intrinsic brain activity (network connectivity) drops around 20 minutes after the stimulation. In this study, all the post-TMS

measurements started within that window thus that effects of TMS interventions should still be detectable. In addition, the averaged pre- and post-TMS interval did not differ across conditions, so we can assume that effects of TMS were comparable between groups.

2.1 TMS intervention modulates GABA concentration

We found a GABA concentration decrease in the occipital cortex after applying inhibitory TMS to the DMN region (lAG) but not after TMS to the parietal region (IPL), with no differences in Glx concentration detected across conditions. It means, that the inhibition of the DMN region reduces the GABA concentration in the visual system. Contrary to our expectation, TMS intervention to the IPL did not affect any neurotransmitter concentration in this area. However, TMS of IPL did decrease iFC inside the visual system along our hypothesis of a top-down effect of IPL.

Few studies reported effects of non-invasive stimulation on neurotransmitter concentrations or neural activity within the same network. Inhibitory theta-burst TMS (iTBS) of the left parietal aspect of the DMN increased GABA concentration in the PCC [120]. Inside the motor system, TMS intervention to the dorsal premotor cortex modulated the neural activity in the contralateral primary motor and dorsal premotor cortices [14]. In addition, local modulation of GABA concentration was reported when applying TMS over extended time periods. In the study by Wang et al., rTMS applied for two weeks in mice increased GABA concentration in prefrontal cortex (PFC) [122]. In the study by Dubin et al., depressed subjects were stimulated by rTMS for 25 days which led to an increase of GABA concentration by 13.8% in the left dorsolateral prefrontal cortex [34]. As shown in these studies, TMS might have a modulatory effect on brain measures distally within the same functional network. Such an effect is not observed if the regions are

not linked. Local inhibitory TMS to the motor cortex modulated GABA concentration in the stimulated spot, but did not affect distant (and functionally unrelated) lentiform nucleus and occipital cortex [77]. In our study, we report for the first time the effect of TMS intervention on the GABA concentration in a sensory brain region located outside the stimulated yet connected functional network.

The underlying mechanism of the TMS-induced GABA modulation is still highly debated. Most reports interpreted the effect as a plasticity-like modulation of the GAD enzyme in GABAergic neurons [77, 109, 112, 117, 120]. As mentioned earlier in section 1.1.1, the downregulation of GAD would be followed by decreased GABA production and release (see Figure 27) and by an increase in Glx concentration. This notion is supported by our results as in the post-TMS_{AG} condition the GABA and Glx correlated negatively, showing that decreased GABA concentration relates to increased Glx concentration.

Besides an effect on GABA concentration, TMS did not have any affect on the Glx/Cr concentration in the occipital cortex. Still, some authors have reported such effects following TMS, but using different stimulation methods. Marjanska et al. observed Glx decrease when stimulating the motor cortex [77]. Others were using transcranial direct stimulation (tDCS) instead of TMS. Applied to the parietal cortex, anodal (excitatory) tDCS elevates Glx in the stimulated region [23], whereas catodal (inhibitory) stimulation decreased Glx in the motor cortex [108]. As we used an inhibitory TMS protocol, this might explain the missing effect on Glx in our study.

We also corrected for several confounding factors in our study. First, as already discussed for Experiment 1 1.1.1, blood flow variations might have an effect on the MRS signal. However, also in this Experiment 2, GABA and Glx FWHM did not significantly differ between conditions. Stable peak widths suggest that the changes in spectra are

caused by modulations in neurotransmitters concentrations. Also, GABA and Glx concentrations were equally distributed across conditions. Second, we corrected for variability in tissue composition of the MRS voxel. Usually, the GABA peak is referenced to the creatine peak (GABA/Cr) in the edited spectrum, but this procedure ignores tissue composition. A recent development in the field is to reference GABA instead to the water peak (GABA/H_2O) [50]. In our study, GABA/H_2O concentration decreased by 20% while GABA/Cr by only 9% after TMS to the lAG. This suggests that water referencing is more accurate in identifying GABA concentration changes as it accounts for tisue specific water signal disproportions. Lastly, we analysed the TMS-specific effect on neurotransmitters compared to other metabolites. In our study, TMS had a specific effect on GABA concentration, but did not affect Glx or other metabolites measured in the spectrum, including Asp, GSH, Ins, PCh, and NAA. However, Marjanska et al. reported that 5-Hz rTMS applied to the motor cortex might decrease at least NAA concentration in the same region [77]. In our study, the NAA concentration was stable across conditions, which suggests that the distal inhibitory rTMS intervention affects only long-range connections and not the local metabolite concentrations.

2.2 Modulation of local and distal neural activity by TMS

In order to better understand the GABAergic TMS-effect of lAG on the visual system, we finally analysed the iFC of lAG to networks of the visual stream (i.e. visual network and DAN). We found that lAG TMS had no effect on the visual network itself but increased DAN iFC. From another analysis not related to this study, we also know that lAG-TMS decreases iFC to DAN and DMN (Castrillon and Riedl, in preparation). In summary, this suggests that lAG TMS decreases the inhibitory effect onto DAN. Others found similar

effects of TMS onto network iFC. In a study by Vidal-Pineiro et al [120], iTBS applied to IPL increased iFC in the DMN. In the study by Antonenko et al., anodal tDCS (at-DCS) applied to the sensorimotor region diminished interhemispheric connectivity of the sensorimotor network. These authors suggested the term *stimulation-induced functional decoupling* for the observed effect of brain stimulation on network-wise iFC changes.

We suggest that TMS to the lAG (as being a part of the DMN) caused functional decoupling of this region from the DMN and the DAN. The disconnection between these two networks increased the iFC inside the DAN. This network is involved in processing of spatial attention, saccade planning and visual working memory [121]. Increased iFC in the DAN might therefore have affected the GABAergic decrease in the visual cortex of post-TMS_{AG} condition.

2.3 Study limitations

In this study, we unfortunately did not assess the effect of inhibitory TMS of the visual cortex on metabolite concentrations and iFC in this region. The reason for this is twofold. First, we observed in preliminary data of an earlier experiment that rTMS stimulation to the occipital cortex did not affect GABA, Glx and other metabolite concentrations (Kurcyus and Riedl, unpublished). Secondly, we were explicitly interested in the distant effects of TMS intervention on functionally connected regions of the brain rather than local TMS effects.

Part VI

Conclusions and Outlook

This thesis investigates the role of the most abundant inhibitory and excitatory neurotransmitters - GABA and Glu - in the visual system. The combination of two methods, MRS and fMRI, allowed relating the levels of neurotransmitters with neuronal activity. Furthermore, we studied the effects of TMS on GABA- and glutamatergic neurotransmission.

One of the remarkable findings of my thesis is that neurotransmitters fluctuate across different brain states in humans. This result is of great importance for the community of MR spectroscopy and suggests that more cautious planning is needed for acquiring MRS data in the future. In **Experiment 1** we observed divergent relationships between the neurotransmitters, neural activity and orientation discrimination performance. These findings might contribute to the understanding of the roles of both molecules in processing visual signals, and their influence on reactivity and sensitivity of the visual system. Glutamate's positive correlation with neural activity during visual stimulation serves as an indicator of the visual system's reactivity. In contrast, the GABA concentration in the same brain state predicted the orientation discrimination performance in the visual task and thus determined the sensitivity of the visual system to detect slight orientation changes in the observed image. It points to a possible function of GABA as a regulator of sensory system distractability [102, 114].

Another important contribution of this thesis is that TMS exerts distant effects on GABA concentration in the visual cortex. To date, TMS was mostly reported to affect neurotransmitter levels and brain activity of the stimulated spot or within the stimulated

network [77, 111, 120]. In **Experiment 2**, we found distant effects of TMS on GABA levels in the occipital cortex. The stimulation did not alter glutamate levels, suggesting that TMS effects on Glx are mainly local, while GABA can be modified distally through long-range connections [31].

In summary, I conclude from the experiments of my thesis that GABA- and Glu-MRS is a novel yet promising technique to study human brain function but still needs more refinement in terms of design and acquisition.

References

[1] Dace Apšvalka, Andrew Gadie, Matthew Clemence, and Paul G Mullins. Event-related dynamics of glutamate and BOLD effects measured using functional magnetic resonance spectroscopy (fMRS) at 3T in a repetition suppression paradigm. *NeuroImage*, 118:292–300, 2015.

[2] Owen J. Arthurs and Simon Boniface. How well do we understand the neural origins of the fMRI BOLD signal? *Trends in Neurosciences*, 25(1):27–31, 2002.

[3] Sawsan As-Sanie, Jieun Kim, Tobias Schmidt-Wilcke, Pia C. Sundgren, Daniel J. Clauw, Vitaly Napadow, and Richard E. Harris. Functional Connectivity Is Associated with Altered Brain Chemistry in Women with Endometriosis-Associated Chronic Pelvic Pain. In *Journal of Pain*, volume 17, pages 1–13, 2016.

[4] Velicia Bachtiar and Charlotte J Stagg. *Interindividual Differences in Behavior and Plasticity*. Elsevier Inc., 2014.

[5] Robert J. Barry, Adam R. Clarke, Stuart J. Johnstone, Christopher A. Magee, and Jacqueline A. Rushby. EEG differences between eyes-closed and eyes-open resting conditions. *Clinical neurophysiology : official journal of the International Federation of Clinical Neurophysiology*, 118(12):2765–73, 2007.

[6] Josef G. Bäuml, Marcel Daamen, Chun Meng, Julia Neitzel, Lukas Scheef, Julia Jaekel, Barbara Busch, Nicole Baumann, Peter Bartmann, Dieter Wolke, Henning Boecker, Afra M. Wohlschläger, and Christian Sorg. Correspondence between aberrant intrinsic network connectivity and gray-matter volume in the ventral brain of preterm born adults. *Cerebral Cortex*, 25(11):4135–4145, nov 2015.

[7] L L Beason-Held, K P Purpura, J W Van Meter, N P Azari, D J Mangot, L M Optican, M J Mentis, G E Alexander, C L Grady, B Horwitz, S I Rapoport, and M B Schapiro. PET reveals occipitotemporal pathway activation during elementary form perception in humans. *Vis Neurosci*, 15(3):503–510, 1998.

[8] William H A Beaudot and Kathy T. Mullen. Orientation discrimination in human vision: Psychophysics and modeling. *Vision Research*, 46(1-2):26–46, 2006.

[9] C.F. Beckmann and S.M. Smith. Probabilistic Independent Component Analysis for Functional Magnetic Resonance Imaging. *IEEE Transactions on Medical Imaging*, 23(2):137–152, feb 2004.

[10] M. Beckmann, H. Johansen-Berg, and M F Rushworth. Connectivity-based parcellation of human cingulate cortex and its relation to functional specialization. *J Neurosci*, 29(4):1175–1190, jan 2009.

[11] Petr Bednarik, Ivan Tkac, Federico Giove, Dinesh K Deelchand, and Silvia Mangia. Correlations between BOLD and neurochemical responses measured in the human visual cortex at 7T. *Proc. Intl. Soc. Mag. Reson. Med.*, 22(8):693, 2014.

[12] Petr Bednařík, Ivan Tkáč, Federico Giove, Mauro DiNuzzo, Dinesh K Deelchand, Uzay E Emir, Lynn E Eberly, and Silvia Mangia. Neurochemical and BOLD responses during neuronal activation measured in the human visual cortex at 7 Tesla. *Journal of cerebral blood flow and metabolism : official journal of the International Society of Cerebral Blood Flow and Metabolism*, 35(4):601–10, 2015.

[13] Graeme I Bell, Toshiaki Kayano, John B Buse, Charles F Burant, Jun Takeda, Denis Lin, Hirofumi Fukumoto, and Susumu Seino. Molecular biology of mammaliam glucose transporters. *Diabetes Care*, 13(3):198–208, 1990.

[14] Sven Bestmann, Orlando Swayne, Felix Blankenburg, Christian C Ruff, Patrick Haggard, Nikolaus Weiskopf, Oliver Josephs, Jon Driver, John C Rothwell, and Nick S Ward. Dorsal premotor cortex exerts state-dependent causal influences on activity in contralateral primary motor and dorsal premotor cortex. *Cerebral Cortex*, 18(6):1281–1291, jun 2008.

[15] Ria Bhola, Evelyn Kinsella, Nicola Giffin, Sue Lipscombe, Fayyaz Ahmed, Mark Weatherall, and Peter J Goadsby. Single-pulse transcranial magnetic stimulation (sTMS) for the acute treatment of migraine: evaluation of outcome data for the UK post market pilot program. *The Journal of Headache and Pain*, 16(1):51, 2015.

[16] David H Brainard. The Psychophysics Toolbox. *Spatial Vision*, 10(4):433–436, 1997.

[17] Joana Cabral, Etienne Hugues, Olaf Sporns, and Gustavo Deco. Role of local network oscillations in resting-state functional connectivity. *NeuroImage*, 57(1):130–139, 2011.

[18] Sarah Cader, Alberto Cifelli, Yasir Abu-Omar, Jacqueline Palace, and Paul M Matthews. Reduced brain functional reserve and altered functional connectivity in patients with multiple sclerosis. *Brain*, 129(2):527–537, oct 2006.

[19] Linda L. Carpenter, Philip G. Janicak, Scott T. Aaronson, Terrence Boyadjis, David G. Brock, Ian A. Cook, David L. Dunner, Karl Lanocha, H. Brent Solvason, and Mark A. Demitrack. Transcranial magnetic stimulation (TMS) for major depression: A multisite, naturalistic, observational study of acute treatment outcomes in clinical practice. *Depression and Anxiety*, 29(7):587–596, jul 2012.

[20] Clara Casco, Michele Barollo, Giulio Contemori, and Luca Battaglini. The effects of aging on orientation discrimination. *Frontiers in Aging Neuroscience*, 9(MAR):45, 2017.

[21] Yan Chao-Gan and Zang Yu-Feng. DPARSF: A MATLAB Toolbox for "Pipeline" Data Analysis of Resting-State fMRI. *Frontiers in systems neuroscience*, 4(May):7, 2010.

[22] In-Young Choi, Sang-Pil Lee, Hellmut Merkle, and Jun Shen. In vivo detection of gray and white matter differences in GABA concentration in the human brain. *NeuroImage*, 33(1):85–93, 2006.

[23] Vincent P. Clark, Brian A. Coffman, Michael C. Trumbo, and Charles Gasparovic. Transcranial direct current stimulation (tDCS) produces localized and specific alterations in neurochemistry: A 1H magnetic resonance spectroscopy study. *Neuroscience Letters*, 500(1):67–71, 2011.

[24] R core Team. R: A language and Environment for statistical computing, 2016.

[25] H. Cousijn, S. Haegens, G. Wallis, J. Near, M. G. Stokes, P. J. Harrison, and A. C. Nobre. Resting GABA and glutamate concentrations do not predict visual gamma frequency or amplitude. *Proceedings of the National Academy of Sciences*, 111(25):9301–9306, 2014.

[26] J S Damoiseaux, S A R B Rombouts, F Barkhof, P Scheltens, C J Stam, S M Smith, and C F Beckmann. Consistent resting-state networks across healthy subjects. *Proceedings of the National Academy of Sciences*, 103(37):13848–13853, 2006.

[27] Niels C. Danbolt. Glutamate uptake. *Progress in Neurobiology*, 65(1):1–105, sep 2001.

[28] Timothy L Davis, Kenneth K Kwong, Robert M Weisskoff, and B. R. Rosen. Calibrated functional MRI: Mapping the dynamics of oxidative metabolism. *Proceedings of the National Academy of Sciences*, 95(4):1834–1839, 1998.

[29] Robin A. de Graaf. *Spectral Editing and 2D NMR*. Elsevier Inc., 2013.

[30] Xin Di, Eun H. Kim, Chu-Chung Huang, Shih-Jen Tsai, Ching-Po Lin, and Bharat B. Biswal. The Influence of the Amplitude of Low-Frequency Fluctuations on Resting-State Functional Connectivity. *Frontiers in Human Neuroscience*, 7(April):118, jan 2013.

[31] Gerald a Dienel, John Byrne, John H. Byrne, and James Lewis Roberts. From Molecules to Networds: An Introduction to Cellular and Molecular Neuroscience. In *An Introduction to Cellular and Molecular Neuroscience*, pages 49–110. Academic Press/Elsevier, 2009.

[32] Manus J. Donahue, Jamie Near, Jakob U. Blicher, and Peter Jezzard. Baseline GABA concentration and fMRI response. *NeuroImage*, 53(2):392–398, nov 2010.

[33] Yuhui Du, Godfrey D. Pearlson, Jingyu Liu, Jing Sui, Qingbao Yu, Hao He, Eduardo Castro, and Vince D. Calhoun. A group ICA based framework for evaluating resting fMRI markers when disease categories are unclear: Application to schizophrenia, bipolar, and schizoaffective disorders. *NeuroImage*, 122:272–280, nov 2015.

[34] Marc J. Dubin, Xiangling Mao, Samprit Banerjee, Zachary Goodman, Kyle A B Lapidus, Guoxin Kang, Conor Liston, and Dikoma C. Shungu. Elevated prefrontal cortex GABA in patients with major depressive disorder after TMS treatment measured with proton magnetic resonance spectroscopy. *Journal of Psychiatry and Neuroscience*, 41(3):E37–E45, 2016.

[35] Serge O. Dumoulin, Alessio Fracasso, Wietske van der Zwaag, Jeroen C.W. Siero, and Natalia Petridou. Ultra-high field MRI: Advancing systems neuroscience towards mesoscopic human brain function. *NeuroImage*, jan 2017.

[36] Richard A E Edden, Suresh D Muthukumaraswamy, Tom C A Freeman, and Krish D Singh. Orientation discrimination performance is predicted by GABA concentration and gamma oscillation frequency in human primary visual cortex. *Journal of Neuroscience*, 29(50):15721–15726, 2009.

[37] Richard A E Edden, Nicolaas A J Puts, Ashley D. Harris, Peter B. Barker, and C. John Evans. Gannet: A batch-processing tool for the quantitative analysis of gamma-aminobutyric acid-edited MR spectroscopy spectra. *Journal of Magnetic Resonance Imaging*, 40(6):1445–1452, nov 2014.

[38] Anna Floyer-Lea. Rapid Modulation of GABA Concentration in Human Sensorimotor Cortex During Motor Learning. *Journal of Neurophysiology*, 95(3):1639–1644, 2006.

[39] Frode Fonnum. Glutamate: A Neurotransmitter in Mammalian Brain. *Journal of Neurochemistry*, 42(1):1–11, jan 1984.

[40] Michael D Fox and Michael Greicius. Clinical applications of resting state functional connectivity. *Frontiers in systems neuroscience*, 4(June):19, jan 2010.

[41] Lei Gao, Lijun Bai, Yuchen Zhang, Xi Jian Dai, Rana Netra, Youjiang Min, Fuqing Zhou, Chen Niu, Wanghuan Dun, Honghan Gong, and Ming Zhang. Frequency-dependent changes of local resting oscillations in sleep-deprived brain. *PLoS ONE*, 10(3), 2015.

[42] Ian Greenhouse, Maedbh King, Sean Noah, Richard J Maddock, and Richard B Ivry. Individual Differences in Resting Corticospinal Excitability Are Correlated with Reaction Time and GABA Content in Motor Cortex. *The Journal of Neuroscience*, 37(10):2686–2696, 2017.

[43] S Groppa, A Oliviero, A Eisen, A Quartarone, L G Cohen, V Mall, A Kaelin-Lang, T Mima, S Rossi, G W Thickbroom, P M Rossini, U Ziemann, J Valls-Solé, and H R Siebner. A practical guide to diagnostic transcranial magnetic stimulation: Report of an IFCN committee, may 2012.

[44] S D Hall, I M Stanford, N Yamawaki, C. J. McAllister, K C Rönnqvist, G L Woodhall, and P L Furlong. The role of GABAergic modulation in motor function related neuronal network activity. *NeuroImage*, 56(3):1506–1510, 2011.

[45] Matti Hämäläinen, Riitta Hari, Risto J. Ilmoniemi, Jukka Knuutila, and Olli V. Lounasmaa. Magnetoencephalography theory, instrumentation, and applications to noninvasive studies of the working human brain. *Reviews of Modern Physics*, 65(2):413–497, 1993.

[46] Michelle Hampson, Fuyuze Tokoglu, Zhongdong Sun, Robin J. Schafer, Pawel Skudlarski, John C. Gore, and R. Todd Constable. Connectivity-behavior analysis reveals that functional connectivity between left BA39 and Broca's area varies with reading ability. *NeuroImage*, 31(2):513–519, jun 2006.

[47] Kihwan Han, Sandra B. Chapman, and Daniel C. Krawczyk. Disrupted Intrinsic Connectivity among Default, Dorsal Attention, and Frontoparietal Control Networks in Individuals with Chronic Traumatic Brain Injury. *Journal of the International Neuropsychological Society*, 22(02):263–279, feb 2016.

[48] Simon Hanslmayr, Alp Aslan, Tobias Staudigl, Wolfgang Klimesch, Christoph S Herrmann, and Karl Heinz Bäuml. Prestimulus oscillations predict visual perception performance between and within subjects. *NeuroImage*, 37(4):1465–1473, 2007.

[49] Ashley D Harris, Nicolaas A J Puts, Brian A Anderson, Steven Yantis, James J Pekar, Peter B Barker, and Richard A E Edden. Multi-Regional Investigation of the Relationship between Functional MRI Blood Oxygenation Level Dependent (BOLD) Activation and GABA Concentration. *PloS one*, 10(2):e0117531, jan 2015.

[50] Ashley D Harris, Nicolaas A J Puts, and Richard A E Edden. Tissue correction for GABA-edited MRS: Considerations of voxel composition, tissue segmentation, and tissue relaxations. *Journal of Magnetic Resonance Imaging*, 42(5):1431–1440, 2015.

[51] Matthew J. Hoptman, Xi Nian Zuo, Pamela D. Butler, Daniel C. Javitt, Debra D'Angelo, Cristina J. Mauro, and Michael P. Milham. Amplitude of low-frequency oscillations in schizophrenia: A resting state fMRI study. *Schizophrenia Research*, 117(1):13–20, mar 2010.

[52] Erik H. Hoyer and Pablo A. Celnik. Understanding and enhancing motor recovery after stroke using transcranial magnetic stimulation. *Restorative Neurology and Neuroscience*, 29(6):395–409, 2011.

[53] Xiao Qi Huang, Su Lui, Wei Deng, Raymond C K Chan, Qi Zhu Wu, Li Jun Jiang, Jun Ran Zhang, Zhi Yun Jia, Xiu Li Li, Fei Li, Long Chen, Tao Li, and Qi Yong Gong. Localization of cerebral functional deficits in treatment-naive, first-episode schizophrenia using resting-state fMRI. *NeuroImage*, 49(4):2901–2906, feb 2010.

[54] Zirui Huang, Henry (Hap) Davis Iv, Qiang Yue, Christine Wiebking, Niall W. Duncan, Jianfeng Zhang, Nils Frederic Wagner, Annemarie Wolff, and Georg Northoff. Increase in glutamate/glutamine concentration in the medial prefrontal cortex during mental imagery: A combined functional mrs and fMRI study. *Human Brain Mapping*, 36(8):3204–3212, aug 2015.

[55] Fahmeed Hyder, Anant B Patel, Albert Gjedde, Douglas L Rothman, Kevin L Behar, and Robert G Shulman. Neuronal–Glial Glucose Oxidation and Glutamatergic–GABAergic Function. *Journal of Cerebral Blood Flow & Metabolism*, 26(7):865–877, jul 2006.

[56] I.Betina Ip, Adam Berrington, Aaron T Hess, Andrew J Parker, Uzay E Emir, and Holly Bridge. Combined fMRI-MRS acquires simultaneous glutamate and BOLD-fMRI signals in the human brain. *NeuroImage*, 2017.

[57] R Jalinous. Technical and practical aspects of magnetic nerve stimulation. *J Clin Neurophysiol*, 8(1):10–25, jan 1991.

[58] Ole Jensen, Bart Gips, Til Ole Bergmann, and Mathilde Bonnefond. Temporal coding organized by coupled alpha and gamma oscillations prioritize visual processing. *Trends in Neurosciences*, 37(7):357–369, 2014.

[59] M. W. Johns, A. Tucker, R. Chapman, K. Crowley, and N. Michael. Monitoring eye and eyelid movements by infrared reflectance oculography to measure drowsiness in drivers. *Somnologie*, 11(4):234–242, nov 2007.

[60] Stephanie R Jones, David J Pinto, Tasso J Kaper, and Nancy Kopell. Alpha-frequency rhythms desynchronize over long cortical distances: A modeling study. *Journal of Computational Neuroscience*, 9(3):271–291, 2000.

[61] Dimitrios Kapogiannis, David A. Reiter, Auriel A. Willette, and Mark P. Mattson. Posteromedial cortex glutamate and GABA predict intrinsic functional connectivity of the default mode network. *NeuroImage*, 64(1):112–119, 2013.

[62] Steffen Katzner, Laura Busse, and Matteo Carandini. GABAA Inhibition Controls Response Gain in Visual Cortex. *Journal of Neuroscience*, 31(16):5931–5941, apr 2011.

[63] James N. C. Kew and John A. Kemp. Ionotropic and metabotropic glutamate receptor structure and pharmacology. *Psychopharmacology*, 179(1):4–29, apr 2005.

[64] Wolfgang Klimesch, Paul Sauseng, and Simon Hanslmayr. EEG alpha oscillations: The inhibition-timing hypothesis. *Brain Research Reviews*, 53(1):63–88, 2007.

[65] Marko Kreft, Lasse K Bak, Helle S Waagepetersen, and Arne Schousboe. Aspects of Astrocyte Energy Metabolism, Amino Acid Neurotransmitter Homoeostasis and Metabolic Compartmentation. *ASN Neuro*, 4(3):AN20120007, apr 2012.

[66] Jan Kujala, Julien Jung, Sandrine Bouvard, Françoise Lecaignard, Amélie Lothe, Romain Bouet, Carolina Ciumas, Philippe Ryvlin, and Karim Jerbi. Gamma oscillations in V1 are correlated with GABAA receptor density: A multi-modal MEG and Flumazenil-PET study. *Scientific Reports*, 5(1):16347, dec 2015.

[67] Bryan H. De La Garza, Eric R. Muir, Guang Li, Yen Yu I Shih, and Timothy Q. Duong. Blood oxygenation level-dependent (BOLD) functional MRI of visual stimulation in the rat retina at 11.7 T. *NMR in Biomedicine*, 24(2):188–193, feb 2011.

[68] Lucien M. Levy, Ulf Ziemann, Robert Chen, and Leonardo G. Cohen. Rapid modulation of GABA in sensorimotor cortex induced by acute deafferentation. *Annals of Neurology*, 52(6):755–761, dec 2002.

[69] Shi-Jiang Li, Zhu Li, Gaohong Wu, Mei-Jie Zhang, Malgorzata Franczak, and Piero G. Antuono. Alzheimer Disease: Evaluation of a Functional MR Imaging Index as a Marker. *Radiology*, 225(1):253–259, oct 2002.

[70] Meng Liang, Yuan Zhou, Tianzi Jiang, Zhening Liu, Lixia Tian, Haihong Liu, and Yihui Hao. Widespread functional disconnectivity in schizophrenia with resting-state functional magnetic resonance imaging. *NeuroReport*, 17(2):209–213, feb 2006.

[71] NK K Logothetis. What we can do and what we cannot do with fMRI. *Nature*, 453(7197):869–78, 2008.

[72] Magor L. Lorincz, Katalin A. Kékesi, Gábor Juhász, Vincenzo Crunelli, and Stuart W. Hughes. Temporal Framing of Thalamic Relay-Mode Firing by Phasic Inhibition during the Alpha Rhythm. *Neuron*, 63(5):683–696, sep 2009.

[73] Mark J. Lowe, Micheal D. Phillips, Joseph T. Lurito, David Mattson, Mario Dzemidzic, and Vincent P. Mathews. Multiple Sclerosis: Low-Frequency Temporal Blood Oxygen Level–Dependent Fluctuations Indicate Reduced Functional Connectivity—Initial Results. *Radiology*, 224(1):184–192, jul 2002.

[74] Silvia Mangia, Federico Giove, and Mauro DiNuzzo. Metabolic pathways and activity-dependent modulation of glutamate concentration in the human brain. *Neurochemical Research*, 37(11):2554–2561, nov 2012.

[75] Silvia Mangia, Ivan Tkáč, Rolf Gruetter, Pierre-Francois Van de Moortele, Bruno Maraviglia, and Kâmil Uğurbil. Sustained Neuronal Activation Raises Oxidative Metabolism to a New Steady-State Level: Evidence from 1H NMR Spectroscopy in the Human Visual Cortex. *Journal of Cerebral Blood Flow & Metabolism*, 27(5):1055–1063, may 2007.

[76] Andrei Manoliu, Valentin Riedl, Anselm Doll, Josef Georg Bäuml, Mark Mühlau, Dirk Schwerthöffer, Martin Scherr, Claus Zimmer, Hans Förstl, Josef Bäuml, Afra M. Wohlschläger, Kathrin Koch, and Christian Sorg. Insular Dysfunction Reflects Altered Between-Network Connectivity and Severity of Negative Symptoms in Schizophrenia during Psychotic Remission. *Frontiers in Human Neuroscience*, 7:216, 2013.

[77] Malgorzata Marjańska, Stéphane Lehéricy, Romain Valabrègue, Traian Popa, Yulia Worbe, Margherita Russo, Edward J Auerbach, David Grabli, Cecilia Bonnet, Cécile Gallea, Mathieu Coudert, Lydia Yahia-Cherif, Marie Vidailhet, and Sabine Meunier. Brain dynamic neurochemical changes in dystonic patients: A magnetic resonance spectroscopy study. *Movement Disorders*, 28(2):201–209, 2013.

[78] Sebastiaan Mathôt, Daniel Schreij, and Jan Theeuwes. OpenSesame: an open-source, graphical experiment builder for the social sciences. *Behavior research methods*, 44(2):314–24, jun 2012.

[79] P M Matthews and P Jezzard. Functional magnetic resonance imaging. *Journal of Neurology, Neurosurgery, and Psychiatry*, 75(1):6–12, 2004.

[80] Ralf Mekle, Simone Kühn, Harald Pfeiffer, Semiha Aydin, Florian Schubert, and Bernd Ittermann. Detection of metabolite changes in response to a varying visual stimulation paradigm using short-TE 1H MRS at 7T. *NMR in Biomedicine*, 30(2):e3672, feb 2017.

[81] M Mescher, H Merkle, J Kirsch, M Garwood, and R Gruetter. Simultaneous in vivo spectral editing and water suppression. *NMR in Biomedicine*, 11(6):266–272, 1998.

[82] Feroze B. Mohamed, Alexander B. Pinus, Scott H. Faro, Dhawal Patel, and Joseph I. Tracy. Bold fMRI of the visual cortex: Quantitative responses measured with a graded stimulus at 1.5 Tesla. *Journal of Magnetic Resonance Imaging*, 16(2):128–136, aug 2002.

[83] Paul G Mullins, David J McGonigle, Ruth L O'Gorman, Nicolaas a J Puts, Rishma Vidyasagar, C John Evans, and Richard a E Edden. Current practice in the use of MEGA-PRESS spectroscopy for the detection of GABA. *NeuroImage*, dec 2012.

[84] Paul G. Mullins, David J. McGonigle, Ruth L. O'Gorman, Nicolaas A J Puts, Rishma Vidyasagar, C. John Evans, Richard A E Edden, Matthew J. Brookes, Adrian Garcia, Bradley R. Foerster, Myria Petrou, Darren Price, Bhavana S. Solanky, Inês R. Violante, Steve Williams, and Martin Wilson. Current practice in the use of MEGA-PRESS spectroscopy for the detection of GABA. *NeuroImage*, 86:43–52, 2014.

[85] Suresh D Muthukumaraswamy, Richard A E Edden, Derek K Jones, Jennifer B Swettenham, and Krish D Singh. Resting GABA concentration predicts peak gamma frequency and fMRI amplitude in response to visual stimulation in humans. *Proceedings of the National Academy of Sciences of the United States of America*, 106(20):8356–8361, 2009.

[86] Fatima A Nasrallah, Julian L Griffin, Vladimir J Balcar, and Caroline Rae. Understanding your inhibitions: modulation of brain cortical metabolism by GABAB receptors. *Journal of Cerebral Blood Flow & Metabolism*, 27(8):1510–1520, aug 2007.

[87] Fatima A. Nasrallah, Julian L. Griffin, Vladimir J. Balcar, and Caroline Rae. Understanding your inhibitions: Effects of GABA and GABAA receptor modulation on brain cortical metabolism. *Journal of Neurochemistry*, 108(1):57–71, jan 2009.

[88] Naohiro Okada, Noriaki Yahata, Daisuke Koshiyama, Kentaro Morita, Kingo Sawada, Sho Kanata, Shinya Fujikawa, Noriko Sugimoto, Rie Toriyama, Mio Masaoka, Shinsuke Koike, Tsuyoshi Araki, Yukiko Kano, Kaori Endo, Syudo Yamasaki, Shuntaro Ando, Atsushi Nishida, Mariko Hiraiwa-Hasegawa, Richard Edden, Peter Barker, Akira Sawa, and Kiyoto Kasai. 592 – GABA and Functional Connectivity in the Anterior Cingulate Cortex in Early Adolescence. *Biological Psychiatry*, 81(10):S239–S240, 2017.

[89] Satu Palva and J Matias Palva. New vistas for α-frequency band oscillations. *Trends in Neurosciences*, 30(4):150–158, 2007.

[90] Anant B Patel, Douglas L Rothman, Gary W Cline, and Kevin L Behar. Glutamine is the major precursor for GABA synthesis in rat neocortex in vivo following acute GABA-transaminase inhibition. *Brain Research*, 919(2):207–220, nov 2001.

[91] R E Paulsen, E Odden, and F Fonnum. Importance of glutamine for gamma-aminobutyric acid synthesis in rat neostriatum in vivo. *Journal of Neurochemistry*, 51(4):1294–9, oct 1988.

[92] Denis G. Pelli. The VideoToolbox software for visual psychophysics: transforming numbers into movies. *Spatial Vision*, 10(4):437–442, 1997.

[93] Russell A. Poldrack, T Nichols, and J Mumford. *Handbook of Functional MRI Data Analysis*. Cambridge University Press, 2011.

[94] Christine Preibisch, J. Gabriel Castrillón G., Martin Bührer, and Valentin Riedl. Evaluation of multiband EPI acquisitions for resting state fMRI. *PLoS ONE*, 10(9), 2015.

[95] Andrew P. Prescot, Allison E. Locatelli, Perry F. Renshaw, and Deborah A. Yurgelun-Todd. Neurochemical alterations in adolescent chronic marijuana smokers: A proton MRS study. *NeuroImage*, 57(1):69–75, 2011.

[96] Stephen W. Provencher. Estimation of metabolite concentrations from localized in vivo proton NMR spectra. *Magnetic Resonance in Medicine*, 30(6):672–679, 1993.

[97] Caroline Rae, Nathan Hare, William A Bubb, Sally R McEwan, Angelika Bröer, James A McQuillan, Vladimir J Balcar, Arthur D Conigrave, and Stefan Bröer. Inhibition of glutamine transport depletes glutamate and GABA neurotransmitter pools: further evidence for metabolic compartmentation. *Journal of neurochemistry*, 85(2):503–514, apr 2003.

[98] Caroline D. Rae. A guide to the metabolic pathways and function of metabolites observed in human brain 1H magnetic resonance spectra. *Neurochemical Research*, 39(1):1–36, 2014.

[99] Marcus E Raichle and Mark a Mintun. Brain work and brain imaging. *Annual review of neuroscience*, 29:449–476, jan 2006.

[100] Juanjuan Ren, Hui Li, Lena Palaniyappan, Hongmei Liu, Jijun Wang, Chunbo Li, and Paolo Maria Rossini. Repetitive transcranial magnetic stimulation versus electroconvulsive therapy for major depression: A systematic review and meta-analysis. *Progress in Neuro-Psychopharmacology and Biological Psychiatry*, 51(Suppl 1):181–189, jun 2014.

[101] V Riedl, K Bienkowska, C Strobel, M Tahmasian, T Grimmer, S Forster, K J Friston, C Sorg, and A Drzezga. Local Activity Determines Functional Connectivity in the Resting Human Brain: A Simultaneous FDG-PET/fMRI Study. *Journal of Neuroscience*, 34(18):6260–6266, apr 2014.

[102] Kristian Sandberg, Jakob Udby Blicher, Mia Yuan Dong, Geraint Rees, Jamie Near, and Ryota Kanai. Occipital GABA correlates with cognitive failures in daily life. *NeuroImage*, 87(100):55–60, feb 2014.

[103] Benoît Schaller, Ralf Mekle, Lijing Xin, Nicolas Kunz, and Rolf Gruetter. Net increase of lactate and glutamate concentration in activated human visual cortex detected with magnetic resonance spectroscopy at 7 tesla. *Journal of Neuroscience Research*, 91(8):1076–1083, aug 2013.

[104] Benoît Schaller, Lijing Xin, Kieran O'Brien, Arthur W. Magill, and Rolf Gruetter. Are glutamate and lactate increases ubiquitous to physiological activation? A 1H functional MR spectroscopy study during motor activation in human brain at 7Tesla. *NeuroImage*, 93(P1):138–145, 2014.

[105] Nicola R Sibson and Kevin L Behar. *Magnetic Resonance Spectroscopy in Neuroenergetics and Neurotransmission*. Elsevier Inc., 2014.

[106] S. M. Smith, P. T. Fox, K. L. Miller, D. C. Glahn, P. M. Fox, C. E. Mackay, N. Filippini, K. E. Watkins, R. Toro, A. R. Laird, and C. F. Beckmann. Correspondence of the brain's functional architecture during activation and rest. *Proceedings of the National Academy of Sciences*, 106(31):13040–13045, aug 2009.

[107] Xiao Wei Song, Zhang Ye Dong, Xiang Yu Long, Su Fang Li, Xi Nian Zuo, Chao Zhe Zhu, Yong He, Chao Gan Yan, and Yu Feng Zang. REST: A Toolkit for resting-state functional magnetic resonance imaging data processing. *PLoS ONE*, 6(9), 2011.

[108] C. J. Stagg, J. G. Best, M. C. Stephenson, J. O'Shea, M. Wylezinska, Z. T. Kincses, P. G. Morris, P. M. Matthews, and H. Johansen-Berg. Polarity-Sensitive Modulation of Cortical Neurotransmitters by Transcranial Stimulation. *Journal of Neuroscience*, 29(16):5202–5206, 2009.

[109] C. J. Stagg, S. Bestmann, A. O. Constantinescu, L. Moreno Moreno, C. Allman, R. Mekle, M. Woolrich, J. Near, H. Johansen-Berg, and J. C. Rothwell. Relationship between physiological measures of excitability and levels of glutamate and GABA in the human motor cortex. *The Journal of Physiology*, 589(23):5845–5855, dec 2011.

[110] Charlotte. Stagg and D. L. Rothman. *Magnetic resonance spectroscopy: tools for neuroscience research and emerging clinical applications*. Academic Press, 2013.

[111] Charlotte J Stagg, Velicia Bachtiar, Ugwechi Amadi, Christel A Gudberg, Andrei S Ilie, Cassandra Sampaio-Baptista, Jacinta O'Shea, Mark Woolrich, Stephen M Smith, Nicola Filippini, Jamie Near, and Heidi Johansen-Berg. Local GABA concentration is related to network-level resting functional connectivity. *eLife*, 2014(3):1–9, 2014.

[112] Charlotte J Stagg, Velicia Bachtiar, and Heidi Johansen-berg. What are we measuring with GABA magnetic resonance spectroscopy? *Commun Integr Biol.*, 4 (5)(October):573–575, 2011.

[113] Jing Sui, Hao He, Qingbao Yu, Jiayu Chen, Jack Rogers, Godfrey D. Pearlson, Andrew Mayer, Juan Bustillo, Jose Canive, and Vince D. Calhoun. Combination of Resting State fMRI, DTI, and sMRI Data to Discriminate Schizophrenia by N-way MCCA + jICA. *Frontiers in Human Neuroscience*, 7:235, 2013.

[114] Petroc Sumner, Richard a E Edden, Aline Bompas, C John Evans, and Krish D Singh. More GABA, less distraction: a neurochemical predictor of motor decision speed. *Nature neuroscience*, 13(7):825–827, jul 2010.

[115] Reggie Taylor, Betsy Schäfer, Maria Densmore, Richard W.J. Neufeld, Nagalingam Rajakumar, Peter C. Williamson, and Jean Théberge. Increased glutamate levels observed upon functional activation in the anterior cingulate cortex using the Stroop Task and functional spectroscopy. *NeuroReport*, 26(3):107–112, feb 2015.

[116] Jan Theeuwes. Perceptual selectivity for color and form. *Perception & Psychophysics*, 51(6):599–606, jun 1992.

[117] S. Tremblay, V. Beaule, S. Proulx, L. de Beaumont, M. Marjanska, J. Doyon, A. Pascual-Leone, M. Lassonde, and H. Theoret. Relationship between transcranial magnetic stimulation measures of intracortical inhibition and spectroscopy measures of GABA and glutamate+glutamine. *Journal of Neurophysiology*, 109(5):1343–1349, 2013.

[118] Kamen A Tsvetanov, Richard N A Henson, Lorraine K Tyler, Adeel Razi, Linda Geerligs, Timothy E Ham, and James B Rowe. Extrinsic and Intrinsic Brain Network Connectivity Maintains

Cognition across the Lifespan Despite Accelerated Decay of Regional Brain Activation. *Journal of Neuroscience*, 36(11):3115–3126, mar 2016.

[119] H. van Dijk, J.-M. Schoffelen, R. Oostenveld, and O. Jensen. Prestimulus Oscillatory Activity in the Alpha Band Predicts Visual Discrimination Ability. *Journal of Neuroscience*, 28(8):1816–1823, 2008.

[120] Dídac Vidal-Piñeiro, Pablo Martín-Trias, Carles Falcón, Núria Bargalló, Imma C Clemente, Josep Valls-Solé, Carme Junqué, Alvaro Pascual-Leone, and David Bartrés-Faz. Neurochemical modulation in posteromedial default-mode network cortex induced by transcranial magnetic stimulation. *Brain Stimulation*, 8(5):937–944, 2015.

[121] S Vossel, J J Geng, and G R Fink. Dorsal and Ventral Attention Systems: Distinct Neural Circuits but Collaborative Roles. *The Neuroscientist*, 20(2):150–159, 2013.

[122] Jinhui Wang, Xinian Zuo, Zhengjia Dai, Mingrui Xia, Zhilian Zhao, Xiaoling Zhao, Jianping Jia, Ying Han, and Yong He. Disrupted functional brain connectome in individuals at risk for Alzheimer's disease. *Biological Psychiatry*, 73(5):472–481, 2013.

[123] Liang Wang, Yufeng Zang, Yong He, Meng Liang, Xinqing Zhang, Lixia Tian, Tao Wu, Tianzi Jiang, and Kuncheng Li. Changes in hippocampal connectivity in the early stages of Alzheimer's disease: Evidence from resting state fMRI. *NeuroImage*, 31(2):496–504, jun 2006.

[124] Heather C. Whalley, Enrico Simonotto, Ian Marshall, David G C Owens, Nigel H Goddard, Eve C Johnstone, and Stephen M Lawrie. Functional disconnectivity in subjects at high genetic risk of schizophrenia. *Brain*, 128(9):2097–2108, sep 2005.

[125] Lirong Yan, Yan Zhuo, Bo Wang, and Danny J J Wang. Loss of Coherence of Low Frequency Fluctuations of BOLD FMRI in Visual Cortex of Healthy Aged Subjects. *The open neuroimaging journal*, 5:105–11, 2011.

[126] Nailin Yao, Shirley Pang, Charlton Cheung, Richard Shek-kwan Chang, Kui Kai Lau, John Suckling, Kevin Yu, Henry Ka-Fung Mak, Grainne McAlonan, Shu-Leong Ho, and Siew-eng Chua. Resting activity in visual and corticostriatal pathways in Parkinson's disease with hallucinations. *Parkinsonism & Related Disorders*, 21(2):131–137, 2015.

[127] B.T. Thomas Yeo, Fenna M. Krienen, Jorge Sepulcre, Mert R. Sabuncu, D. Lashkari, Marisa Hollinshead, Joshua L. Roffman, Jordan W. Smoller, Lilla Zollei, Jonathan R. Polimeni, Bruce Fischl, Hesheng Liu, and Randy L. Buckner. The organization of the human cerebral cortex estimated by intrinsic functional connectivity. *Journal of neurophysiology*, 106:1125–1165, 2011.

[128] Jong H Yoon, Richard J Maddock, Ariel Rokem, Michael A Silver, Michael J Minzenberg, J Daniel Ragland, and Cameron S Carter. GABA Concentration Is Reduced in Visual Cortex in Schizophrenia and Correlates with Orientation-Specific Surround Suppression. *Journal of Neuroscience*, 30(10):3777–3781, 2010.

[129] Yu Feng Zang, Yong He, Chao Zhe Zhu, Qing Jiu Cao, Man Qiu Sui, Meng Liang, Li Xia Tian, Tian Zi Jiang, and Yu Feng Wang. Altered baseline brain activity in children with ADHD revealed by resting-state functional MRI 375. *Brain & development*, 29(2):83–91, 2007.

[130] Xiaoliu Zhang, Yingying Tang, Mirjana Maletic-Savatic, Jianhua Sheng, Xuanhong Zhang, Yajing Zhu, Tianhong Zhang, Junjie Wang, Shanbao Tong, Jijun Wang, and Yao Li. Altered neuronal spontaneous activity correlates with glutamate concentration in medial prefrontal cortex of major depressed females: An fMRI-MRS study. *Journal of Affective Disorders*, 201:153–161, 2016.

Part VII

Publications

1 Publications derived from this thesis

Different baseline states of GABA and Glx in the human brain and their relation to visual input processing.

Kurcyus K, Annac E, Henning N, Oeltzschner G, Pilatus U, Edden R, Riedl V. In preparation.

GABA and intrinsic connectivity changes in the visual system induced by repetitive inhibitory transcranial magnetic stimulation.

Kurcyus K, Castrillon G, Sollmann N, Krieg S, Edden R, Riedl V. In preparation.

2 Publications, which are not part of this thesis

Local Activity Determines Functional Connectivity in the Resting Human Brain: A Simultaneous FDG-PET/fMRI Study.

Riedl V, Bienkowska K, Strobel C, Tahmasian M, Grimmer T, Forster S, Friston KJ, Sorg C, Drzezga A. Journal of Neuroscience, 34(18):6260–6266, April 2014.

3 Oral presentations derived from this thesis

Correlation of GABA and glutamate levels with resting-state intrinsic functional connectivity (iFC) of the human visual system.

Kurcyus K, Riedl V. 2nd International Symposium on MRS of GABA, Cardiff, UK, September 2013.

The metabolic foundation of intrinsic brain activity.

Kurcyus K, Riedl V. 64th Lindau Nobel Laureate Meeting in Medicine and Physiology, Lindau, Germany, July 2014.

Downstream effects of repetitive inhibitory TMS on GABA and GSH levels.

Kurcyus K, Castrillon G, Sollmann N, Krieg S, Edden R, Riedl V. 3rd International Symposium on MRS of GABA, Orlando, FL, October 2015. **Award of best student presentation received.**

4 Poster presentations derived from this thesis

GABA and Glu levels correlation with intrinsic functional connectivity (iFC) of the visual system.

Kurcyus K, Riedl V. 20th Annual Meeting of the Organisation of Human Brain Mapping, Hamburg, Germany, June 2014.

Local intrinsic connectivity measures relate to GABA/Glx levels.

Kurcyus K, Riedl V. 23rd International Society of Magnetic Resonance in Medicine Meeting in Toronto, Canada, May, 2015.

GABA changes can be induced by state and external (TMS) modulation, and tracked dynamically with MRS.

Kurcyus K, Castrillon G, Sollmann N, Krieg S, Edden R, Riedl V. 22nd Annual Meeting of the Organisation of Human Brain Mapping in Geneva, Switzerland, June 2016.

Part VIII

Acknowledgements

I would like to express my greatest appreciation to my supervisor Dr. Valentin Riedl for his generous and enthusiastic support I received from him in last couple of years. His extraordinary and creative personality makes him a brilliant researcher and an inspirational mentor. His empathetic and encouraging attitude helped me to reach goals I was not even able to perceive.

Advices given by Prof. Dr. Markus Ploner and Prof. Dr. Helmut Adelsberger, who were members of my thesis committee, have been a great help in critical evaluation of my results and guided me to see my scientific work from many perspectives.

I would like to thank Prof. Dr. Zimmer and Prof. Dr. Schwaiger for providing me with the opportunity to perform my experiments in the Departments of Neuroradiology and Nuclear Medicine of the Klinikum rechts der Isar, which research infrastructure and scientific environment with many exceptional scientists and students are of tremendous value. Without these facilities writing this thesis could not have been possible.

I wish to acknowledge the help provided by coordinators of MLST Program, Ms. Desislava Zlatanova and Dr. Katrin Offe and also by our secretary, Ms. Sigrid Matusek. Their friendly and patient support with administrative and academic tasks throughout my graduate studies were priceless.

I am particularly grateful for the assistance with the data collection given by Sylvia Schachoff, Anna Winter and Claudia Meisinger. They taught me how to acquire the neuroimaging data and always helped me when needed. They simply do their jobs great.

My work time would not be so enjoyable and rewarding without colleagues and friends

from the Department of Neuroradiology. Thank you Gabriel, Lukas and Miguel for making my daily life in the office amusing. Thank you Georgiana and Martina for your friendship and many extracurricular activities. Thank you Aurore, Monica, Deniz, Joseph, Tim, Moritz and Son for many pleasant breaks from work. Masoud, Judita, Marie-Luise, Chun and Lorenzo are not around anymore, but their good vibes are still noticeable.

My thanks are extended to the two exceptional teachers I have encountered in my high school, Marcin Wierzba and Dr. Tomasz Maltz. Their passion about science awaken my curiosity for nature and human brain and made me pursue the carrier in academia. I would not have been where I am right now without them.

I would like to offer my special thanks to the DAAD, an organization that enabled me to study in Munich. It would not be feasible without their support. Another great opportunity was given to me by the Elite Network of Bavaria who supported my participation in the Nobel Laureates Meeting in Lindau. It was a truly amazing experience to meet the most distinguishable researchers of those times.

I would like to thank my family and friends, especially my beloved Mother, whose love and infinite support in reaching my goals encouraged me to move to Germany and eventually graduate from one of the best Universities in the world. Her strength and ambition also encouraged me to go off the beaten path.

Lastly, my life would not have been painted with the same colors without my beloved husband, whose support in good and tough times is inestimable. His optimistic attitude dissolves all the problems on our way and makes me praise every moment we spend together.